

# Ginsburg-Landau theory of solid and supersolid and their applications to ${}^4\text{He}$

Jinwu Ye

Department of Physics, The Pennsylvania State University, University Park, PA, 16802

(Dated: February 8, 2020)

We construct a Ginsburg Landau (GL) theory to map out the  ${}^4\text{He}$  phase diagram, analyze the conditions for the existence of the supersolid (SS) and study all the phases and phase transitions in a unified framework. Depending on the sign and strength of the repulsive coupling between the normal solid (NS) and superfluid (SF) in the GL theory, there are two scenarios (1) If it is larger than a critical value, then No SS exists. Then for the first time, we construct a quantum Ginsburg-Landau theory (QGL) to study the SF to NS transition and explicitly derive the Feymann relation from the QGL (2) If it is smaller than the critical value, then a SS exists at sufficient low temperature. If the coupling is negative ( positive ), the SS is due to vacancy ( interstitial ) condensation and named SS-v ( SS-i ). In scenario (2), by increasing the pressure from the superfluid side, the superfluid to supersolid (SS) transition is a simultaneous combination of first order transitions of superfluid density wave ( SDW) formation in the superfluid sector driven by the roton condensation and NS formation in the normal density sector driven by the divergence of structure function. For vacancies induced supersolid (SS-v), the SDW coincides with the normal lattices, while for interstitials induced supersolid (SS-i), the SDW takes the dual lattices of the normal lattices. We also investigate the SS from the NS side and find the transition is described by a 3d  $XY$  with much *narrower* critical regime than the conventional NL to the SF transition. This fact is responsible for the extreme sensitivity to even tiny concentration of  ${}^3\text{He}$  impurities. The X-ray scattering intensity from the SS-v is the same as that from the NS at mean field level, but will differ when the Deybe-Waller factor is taken into account. The X-ray scattering intensity from the SS-i ought to have an additional modulation over that of the NS even at mean field level. The modulation amplitude is proportional to the Non-Classical Rotational-Inertial (NCRI) observed in the torsional oscillator experiments. The X-ray scattering patterns from different lattice structure structures of SS-i are derived. The important effects of Deybe-Waller factor on X-ray scattering in both SS-v and SS-i are stressed. The NCRI in the SS state is calculated and found to be isotropic in *bcc* and *fcc* lattice, but weakly anisotropic in *hcp* lattice. All the low energy excitations in the SS phases are discussed. The applications to solid Hydrogen and bilayer electronic systems are discussed. Comparisons with the lattice supersolid are made. We also make comments on other experiments.

## I. INTRODUCTION

A solid can not flow. It breaks a continuous translational symmetry into a discrete lattice translational symmetry. There are low energy lattice phonon excitations in the solid. While a superfluid can flow even through narrowest channels without any resistance. It breaks a global  $U(1)$  phase rotational symmetry and has the off-diagonal long range order (ODLRO)<sup>1</sup>. There are low energy superfluid phonon excitations in the superfluid. A supersolid is a state which has both the ODLRO and crystalline order. The possibility of a supersolid phase in  ${}^4\text{He}$  was theoretically speculated in 1970<sup>2,3,4,5</sup>. Andreev and Lifshitz proposed the Bose condensation of vacancies as the mechanism of the formation of supersolid<sup>2</sup>. Chester wrote down a wavefunction which has both ODLRO and crystalline order and also speculated that a supersolid cannot exist without vacancies or interstitial<sup>3</sup>. Leggett proposed that solid  ${}^4\text{He}$  might display Non-Classical Rotational Inertial (NCRI) which is a low temperature reduction in the rotational moment of inertia due to the superfluid component of solid  ${}^4\text{He}$ <sup>4,5,6</sup>. Leggett also suggested that quantum tunneling of He atoms between neighboring sites in a crystal can also lead to a supersolid even in the absence of vacancies. Over the last 35 years, a number of experiments have been designed to search for

the supersolid state without success. However, recently, by using torsional oscillator measurement, a PSU group lead by Chan observed a marked  $1 \sim 2\%$  NCRI of solid  ${}^4\text{He}$  at  $\sim 0.2\text{K}$ , both when embedded in Vycor glass<sup>7</sup> and in bulk  ${}^4\text{He}$ <sup>8</sup>. Some of the important experimental facts are:(1) the NCRI slides towards the normal solid regime with a very long tail. (2) the superfluid fraction has a non-monotonic dependence on the pressure, it increases first, reaches a maximum at  $\sim 55\text{ bar}$ , then decreases to zero at a much higher pressure  $p_{c2} \sim 170\text{ bar}$ <sup>10</sup>. (3) the supersolid has a very low critical velocity corresponding to  $\sim 1 - 3$  flux quanta above which the NCRI is reduced (4) a very tiny fraction of  $\text{He3}$  in the range of  $x \sim 40\text{ppB} - 85\text{ppM}$  decreases the superfluid fractions, but increases the supersolid to normal solid transition temperature considerably<sup>11</sup>. This observation is very counter-intuitive and in sharp contrast to the effects of He3 impurities in both 3d  ${}^4\text{He}$  superfluid and 2d superfluid  ${}^4\text{He}$  films. (5) Although the previous experiment at  ${}^3\text{He}$  impurities concentration  $x \sim 30\text{ ppM}$  to temperature as low as  $100\text{mK}$  did not detect any obvious specific anomaly<sup>9</sup>, recent much more refined experiments in the range  $x \sim 0.3 - 3\text{ ppM}$  to temperature as low as  $45\text{ mK}$  showed that an excessive specific heat shows a broad peak around the putative supersolid onset critical temperature  $\sim 100\text{ mK}$ <sup>11</sup>. The authors suggested that

the supersolid state of  ${}^4\text{He}$  maybe responsible for the NCRI. They mapped out the experimental global phase diagram of  ${}^4\text{He}$  in the Fig.4 in<sup>8</sup>. More recently, the PSU group detected about  $10^{-4}$  reduction in the rotational inertial, but by performing blocked cell experiments, the authors concluded that the reduction is *classical* due to the motion of  $HD$  impurities clustering. So the PSU group did not find any NCRI in solid hydrogen<sup>11</sup>.

The PSU experiments forced us to reexamine the already fantastic physics in  ${}^4\text{He}$  and rekindled extensive both theoretical<sup>12,13,14,15</sup> and experimental<sup>16,17</sup> interests in the still controversial supersolid phase of  ${}^4\text{He}$ . There are two kinds of complementary theoretical approaches. The first is the microscopic numerical simulation<sup>12</sup>. The second is the phenomenological approach<sup>13,15</sup>. At this moment, despite all the theoretical work, there is no consensus at all on the interpretation of PSU's experiments. In this paper, we will construct a phenomenological Ginsburg Landau (GL) theory to study all the possible phases and phase transitions in helium 4 system. We identify order parameters, symmetry and symmetry breaking patterns in all the phases. Particularly, we will address the following two questions: (1) What is the condition for the existence of the SS state? (2) If the SS exists, what are the properties of the supersolid to be tested by possible new experiments.

Let's start by reviewing all the known phases in  ${}^4\text{He}$ . The density of a normal solid (NS) is defined as  $n(\vec{x}) = n_0 + \sum_{\vec{G}} n_{\vec{G}} e^{i\vec{G}\cdot\vec{x}}$  where  $n_{\vec{G}}^* = n_{-\vec{G}}$  and  $\vec{G}$  is any non-zero reciprocal lattice vector. In a normal liquid (NL), if the static liquid structure factor  $S(k)$  has its first maximum peak at  $\vec{k}_n$ , then near  $k_n$ ,  $S(k) \sim \frac{1}{r_n + c(k^2 - k_n^2)^2}$ . If the liquid-solid transition is weakly first order, it is known that the classical free energy to describe the NL-NS transition is<sup>18,26</sup>:

$$f_n = \sum_{\vec{G}} \frac{1}{2} r_{\vec{G}} |n_{\vec{G}}|^2 - w \sum_{\vec{G}_1, \vec{G}_2, \vec{G}_3} n_{\vec{G}_1} n_{\vec{G}_2} n_{\vec{G}_3} \delta_{\vec{G}_1 + \vec{G}_2 + \vec{G}_3, 0} + u \sum_{\vec{G}_1, \vec{G}_2, \vec{G}_3, \vec{G}_4} n_{\vec{G}_1} n_{\vec{G}_2} n_{\vec{G}_3} n_{\vec{G}_4} \delta_{\vec{G}_1 + \vec{G}_2 + \vec{G}_3 + \vec{G}_4, 0} + (1)$$

where  $r_{\vec{G}} = r_n + c(G^2 - k_0^2)^2$  is the tuning parameter controlled by the pressure. The GL parameters  $w$  and  $u$  may be determined by fitting the theoretical predictions with experimental data. It is easy to see that Eqn.1 is invariant under  $\vec{x} \rightarrow \vec{x} + \vec{a}$ ,  $n(\vec{x}) \rightarrow n(\vec{x} + \vec{a})$ ,  $n(\vec{G}) \rightarrow n(\vec{G}) e^{i\vec{G}\cdot\vec{a}}$  where  $\vec{a}$  is any vector. In the NL,  $n(\vec{G}) = 0$ , the translational symmetry is respected. In the NS,  $n(\vec{G}) \neq 0$ , the symmetry is broken down to translational invariance under only a lattice constant  $\vec{a} = \vec{R}$ ,  $\vec{G} \cdot \vec{R} = 2\pi n$ ,  $n(\vec{x}) \rightarrow n(\vec{x} + \vec{R})$ ,  $n(\vec{G}) \rightarrow n(\vec{G})$ . As shown in the Fig.2, the NL to NS transition only happens at finite temperature, so the classical theory is valid. Note that due to the *lack* of the  $Z_2$  symmetry of  $n_{\vec{G}} \rightarrow -n_{\vec{G}}$ , there is always a cubic term which makes the the NL to NS a 1st order transition. Quantum fluctuations can be incorporated by  $n(\vec{x}) \rightarrow n(\vec{x}, \tau)$  and including  $\frac{1}{2}\rho_n(\partial_\tau n)^2$  in Eqn.1.

Of course, the Superfluid to Normal Liquid transition at finite temperature in the Fig.2 is the 3d XY transition described by<sup>24</sup>:

$$f_\psi = K|\nabla\psi|^2 + t|\psi|^2 + u|\psi|^4 + \dots \quad (2)$$

where  $\psi$  is the complex order parameter and  $t$  is the tuning parameter controlled by the temperature. Eqn.2 is invariant under the global  $U(1)$  symmetry  $\psi \rightarrow \psi e^{i\theta}$ . In the NL,  $\langle \psi \rangle = 0$ , the symmetry is respected. In the SF,  $\langle \psi \rangle \neq 0$ , the symmetry is broken. The GL parameters  $K, t, u$  may be determined by fitting the theoretical predictions with experimental data. Quantum fluctuations can be included by  $\psi(\vec{x}) \rightarrow \psi(\vec{x}, \tau)$  and including  $\psi^\dagger(\vec{x}, \tau)\partial_\tau\psi(\vec{x}, \tau)$  in Eqn.2.

The coupling between  $n(\vec{x})$  and  $\psi(\vec{x})$  consistent with all the symmetry can be written down as:

$$f_{int} = v_1 n(\vec{x}) |\psi(\vec{x})|^2 + \dots \quad (3)$$

where due to the two competing orders between the solid and the superfluid, we expect the coupling is attractive  $v_1 = v_v < 0$  for vacancies, but repulsive  $v_1 = v_i$  for interstitials. As shown in section V, the repulsive interaction is crucial to shift down the normal solid to the supersolid transition temperature in the Fig.3. In fact, the temperature shift  $T_{SF} - T_{SS-i}$  is proportional to the repulsive strength  $v_i$ . The  $\dots$  include terms like  $v_2 n^2(\vec{x}) |\psi(\vec{x})|^2 + w_1 n(\vec{x}) |\nabla\psi(\vec{x})|^2 + \dots$  which are sub-leading to the  $v_1$  term and can be neglected at the mean field level to be analyzed in this paper. Eqn.3 is invariant under both the translational symmetry  $\vec{x} \rightarrow \vec{x} + \vec{a}$ ,  $n(\vec{x}) \rightarrow n(\vec{x} + \vec{a})$ ,  $\psi(\vec{x}) \rightarrow \psi(\vec{x} + \vec{a})$  and the global  $U(1)$  symmetry  $\psi \rightarrow \psi e^{i\theta}$ .

Due to the lack of particle-hole symmetry in the normal solid, quantum fluctuations can be included by additional terms like  $n(\vec{x}, \tau)\psi^\dagger(\vec{x}, \tau)\partial_\tau\psi(\vec{x}, \tau)$  in Eqn. 3. We will explicitly consider the quantum fluctuations in sections II and III where we will discuss superfluid density wave formation in  $\psi$  sector only and in section IV where we will discuss the quantum phase transition from the superfluid to the solid. In the rest of the paper, we only perform our calculations at mean field level inside a given phase, then all the  $\tau$  derivative terms can be neglected. However, they are very important to determine the low energy excitation spectra in a given phase and will be investigated in<sup>27</sup>. In all the classical phase transitions addressed in this paper, we will also neglect these quantum fluctuation terms. However, they are very important in the zero temperature quantum phase transition from SS to NS driven by the pressure ( see Fig.3 ) and will be investigated in<sup>27</sup>.

A solid has the order in the number density, while a superfluid has the order in the phase. The two phases are in totally different extremes of the state of matter. How to combine the two opposite extremes into a novel state of matter, supersolid, is an important and interesting topic. It is widely believed that the only chance to get a supersolid is that the solid is not *perfect*, namely, it

is an incommensurate solid which has defects such as vacancies or interstitials, so the total number of bosons can fluctuate to give some rooms for the invasion of superfluid. Due to large zero point motions, there are indeed rapid exchanging between local  ${}^4\text{He}$  atoms in bulk  ${}^4\text{He}$ , but this local process is unlikely to lead to a global phase ordering. It was estimated from both X-ray scattering experiments<sup>33</sup> and some microscopic calculations<sup>12</sup> that the thermal excitation energies of a vacancy and interstitial are  $E_v \sim 10 K, E_i \sim 40 K$ , so thermal fluctuations favor vacancies over interstitials. Because both have very high energy, so the thermal generated vacancies and interstitials are irrelevant around  $200 mK$ . However, it is still possible that there are quantum fluctuation generated vacancies and interstitials even at  $T = 0$ . It is still not known if quantum fluctuations favor vacancies over interstitials or not<sup>15</sup>. In fact, due to the very peculiar potential well in the solid  ${}^4\text{He}$  which has a local shallow maximum at the lattice site, it is possible that the quantum fluctuations may even favor interstitials over vacancies. So in this paper, to be complete, we study both cases. We call vacancies induced supersolid as SS-v, interstitials induced supersolid as SS-i. When the two kinds of SS show different properties, we treat them differently, when they share the same properties, we treat them just in the same notation SS.

In an effective GL theory,  $n(\vec{x})$  and  $\psi(\vec{x})$  emerge as two independent order parameters. In SS-v and SS-i,  $\psi(\vec{x})$  stands for vacancies and interstitials respectively. The total density of the system is  $n_t(x) = n(x) + |\psi(x)|^2$  where  $n(x)$  is the normal density and  $|\psi(x)|^2$  is the superfluid density. This relation is straightforward for interstitials. For vacancies, if all the vacancies are in the normal state, then the solid's density is defined as  $n_t(x)$ , then the relation also holds. The GL equations 1,2,3 are invariant under both the translational symmetry  $\vec{x} \rightarrow \vec{x} + \vec{a}, n(\vec{x}) \rightarrow n(\vec{x} + \vec{a}), n(\vec{G}) \rightarrow n(\vec{G})e^{i\vec{G}\cdot\vec{a}}, \psi(\vec{x}) \rightarrow \psi(\vec{x} + \vec{a})$  and the global  $U(1)$  symmetry  $\psi \rightarrow \psi e^{i\theta}$ . In a NL,  $n_{\vec{G}} = 0, \langle \psi \rangle = 0$ . In a SF,  $n_{\vec{G}} = 0, \langle \psi \rangle \neq 0$ . In a NS,  $n_{\vec{G}} \neq 0, \langle \psi \rangle = 0$ , while in a supersolid,  $n_{\vec{G}} \neq 0, \langle \psi \rangle \neq 0$ . From the normal liquid ( NL ) side, one can approach both the solid and the superfluid. Inside the NL,  $t > 0$ ,  $\psi$  has a gap, so can be integrated out, we recover the solid-liquid transition tuned by  $r_{\vec{G}}$  in Eqn.1 ( Fig.3 ). Inside the NL  $\langle n(\vec{x}) \rangle = n_0$ , so we can set  $n_{\vec{G}} = 0$  for  $\vec{G} \neq 0$  in Eqn.3, then we recover the NL to SF transition tuned by  $t$  in Eqn.2 ( Fig.2 ).

Although the NL-NS and NL-SF transitions are well understood, so far, the SF-NS transition has not been investigated seriously. This transition may be in a completely different universality class than the NL-NS transition, because both sides break two completely different symmetry: internal global  $U(1)$  symmetry and translational ( and orientational ) symmetry. It is possible that the solid reached from the SF side is a new kind of solid than the NS reached from the NL side. In a recent paper<sup>20</sup>, we constructed a simple, novel and powerful two components quantum Ginsburg Landau (QGL) theory in

the  $\psi$  sector to study superfluid density wave formation transitions in the superfluid. As shown in<sup>20</sup>, the problem of studying superfluid density wave formation inside a superfluid state is interesting on its own. In this paper, using the QGL theory developed in<sup>20</sup> and incorporating the attractive or repulsive coupling between  $\psi$  and  $n$  sector in Eqn.3, we determine the global  ${}^4\text{He}$  phase diagram and study all the phases and phase transitions in a *unified framework*. We develop the theory starting from the two facts (1) there is a roton minimum in the superfluid state (2) The instability to solid formation is driven by the gap diminishing at the roton minimum. The fact (1) was well established. The fact (2) also has some earlier theoretical and experimental supports ( see<sup>21,22</sup> and references therein). If the coupling in Eqn.3 is negative, the system is always in a SS-v ( Fig.1). If it is positive, then only when it is smaller than a critical value, a SS-i state will appear, otherwise the system is in the NS ( Fig.1 ). The resulting solid at high pressure could be an incommensurate solid with zero point quantum fluctuations generated vacancies or interstitials whose condensation leads to the formation of the SS-v and SS-i respectively. The SS phase naturally and consistently fits into the phase diagram. The theory can be used to address several important phenomena observed in the PSU experiments and also make sharp predictions to be tested by possible future experiments, especially X-ray scattering experiments in the SS state. Our main results on supersolid are independent of many microscopic details, should be universal and may have some applications on PSU's experiments on  ${}^4\text{He}$  and other systems.

The rest of the paper is organized as the following: In Sec. II, we rephrase the two component QGL theory in the  $\psi$  sector developed in<sup>20</sup> using  ${}^4\text{He}$  superfluid notations. In sec.III, we use the QGL theory to study the superfluid to superfluid density wave (SDW) transition driven by the roton condensation at  $k = k_r$  in the  $\psi$  sector alone which is interesting on its own. In sec. IV, for the first time, we construct a quantum Ginsburg-Landau action to study SF to the NS transition and also explicitly establish the Feymann relation from the QGL. In Sec.V, taking into account the coupling between the  $n$  and  $\psi$  sector encoded in Eqn.3, we study the superfluid to supersolid transition which is a simultaneous combination of the SDW transition in  $\psi$  sector driven by the roton condensation at  $k_0 = k_r$ , discussed in Sec. III and the NS transition in the  $n$  sector driven by the divergence of the structure function at  $k_0 = k_r = k_n$  discussed in Sec.IV. We also sketch the global phase diagrams to be confirmed and analyzed in the following sections. In Sec.VI, we approach the SS phase from the NS side and discuss the SDW in SS-v and SS-i respectively. We also classify several common SS lattice structures. In Sec. VII, we make key predictions on the elastic X-ray scattering amplitudes from all SS-v and SS-i structures classified in Sec. VI. These predictions are amenable to ongoing X-ray scattering experiments at PSU<sup>11</sup>. In Sec. VIII, we calculate the NCRIs in both the SF and SS states and find the

NCRI in the *hcp* SS lattice may be weakly anisotropic. In Sec. IX, we discuss all the low energy excitations in the SS state and also estimate the very large vortex size and low critical velocity in the supersolid state. In Sec. X, we apply our theory to analyze the PSU's experiments in  ${}^4\text{He}$ , especially the dramatic effects of He3 impurities and also comment on several other experiments. We also compare the properties of the SS with those of lattice SS on extended boson Hubbard model. The applications of the GL theory on Hydrogen and fermionic systems such as bilayer quantum Hall systems and electron-hole bilayer systems are also briefly mentioned. Conclusions are summarized in the final section IX. In the appendix, we discuss the properties of a *toy* SS-v wavefunction. A short report of these results appeared in<sup>23</sup> where the X-ray scattering from SS-i is emphasized.

## II. TWO-COMPONENT QGL THEORY IN THE $\psi$ SECTOR

The superfluid is described by a complex order parameter  $\psi$  whose *condensation* leads to the Landau's quasi-particles. Although the bare  ${}^4\text{He}$  atoms are strongly interacting, the Landau's quasi-particles are weakly interacting. Usually,  $\psi$  describes fluctuations near  $k = 0$ , while a superfluid density wave (SDW) is described by a density operator  $\rho$  which sets up a lattice scale at  $k \sim 1/a$  where  $a$  is the lattice constant. In order to describe both superfluid and superfluid density wave on the same footing by a QGL theory, we will take the  $\psi$  as the primary order parameter, while the superfluid density operator  $\rho = |\psi|^2$  just as a descendent ( or derivative ) order parameter. Note that  $\rho$  is different from  $n(x)$  in Eqn.1 which should be taken as an independent variable in the effective GL theory. This indicates that the resulting SDW not only has the conventional translational and rotational orders characterized by  $\rho$ , also has a quantum phase order characterized by the more fundamental order parameter  $\psi$ . The most general Quantum Ginsburg-Landau (QGL) action at any dimension, any pressure and any temperature to supersede Eqn.2 is:

$$\begin{aligned} \mathcal{S}_\psi = & \frac{1}{2} \int d^d x d\tau [\psi^\dagger \partial_\tau \psi + \kappa |\partial_\tau \psi|^2 + t |\psi|^2 + K |\nabla \psi|^2 \\ & + L_1 |\nabla^2 \psi|^2 + L_2 |\nabla^3 \psi|^2] + u \int d^d x d\tau |\psi(\vec{x}, \tau)|^4 + (4) \end{aligned}$$

In the following, for simplicity, we neglect the linear derivative terms, major physics in the  $\psi$  sector stays the same if this term is included.

The above equation generalize Eqn.2 to include the strong long-range interaction between  ${}^4\text{He}$  atoms which are incorporated into  $L_1, L_2$  terms, the residue short-range interaction  $u$  is weak, so a perturbative expansion in terms of  $u$  is possible. The hard core and long-range Lennard-Jones potential between  ${}^4\text{He}$  atoms lead to  $L_1 < 0, L_2 > 0$  in the superfluid state where  $t < 0$ .

This fact, in turn, leads to the dispersion curve of superfluid state  $\omega^2 = Kq^2 - |L_1|q^4 + L_2q^6$  ( see also Eqn.13 ) shown in Fig. 1 b which has both a phonon sector and a roton sector. In order to focus on the low energy modes, we divide the spectrum into two regimes: the low momenta regime  $k < \Lambda$  where there are phonon excitations with linear dispersion and high momentum regime  $|k - k_r| < \Lambda \ll k_r$  where there is a roton minimum at the roton surface  $k = k_r$ . We separate the complex order parameters  $\psi(\vec{x}, \tau) = \psi_1(\vec{x}, \tau) + \psi_2(\vec{x}, \tau)$  into  $\psi_1(\vec{x}, \tau) = \int_0^\Lambda \frac{d^d k}{(2\pi)^d} e^{i\vec{k}\cdot\vec{x}} \psi(\vec{k}, \tau)$  and  $\psi_2(\vec{x}, \tau) = \int_{|k-k_r|<\Lambda} \frac{d^d k}{(2\pi)^d} e^{i\vec{k}\cdot\vec{x}} \psi(\vec{k}, \tau)$  which stand for low energy modes near the origin and  $k_r$  respectively. For the notation simplicity, in the following,  $\int_\Lambda$  means  $\int_{|k-k_r|<\Lambda}$ . The GL action in the  $(\vec{k}, \omega)$  space becomes:

$$\begin{aligned} \mathcal{S}_\psi = & \frac{1}{2} \int_0^\Lambda \frac{d^d k}{(2\pi)^d} \frac{1}{\beta} \sum_{i\omega_n} (\kappa \omega_n^2 + t + K k^2) |\psi_1(\vec{k}, i\omega_n)|^2 \\ & + \frac{1}{2} \int_\Lambda \frac{d^d k}{(2\pi)^d} \frac{1}{\beta} \sum_{i\omega_n} (\kappa \omega_n^2 + \Delta_r + v_r (k - k_r)^2) |\psi_2(\vec{k}, i\omega_n)|^2 \\ & + u \int d^d x d\tau |\psi_1(\vec{x}, \tau) + \psi_2(\vec{x}, \tau)|^4 + \dots \end{aligned} \quad (5)$$

where  $\kappa$  is the compressibility,  $t \sim T - T_c$  where  $T_c \sim 2.17K$  is the critical temperature of superfluid to normal fluid transition at  $p = 0.05 \text{ bar}$  and  $\Delta_r \sim p_{c1} - p$  where  $p_{c1} \sim 25 \text{ bar}$  is the critical pressure of superfluid to the supersolid transition at  $T = 0$ .

The fact that the spectrum in the superfluid state has low energy modes at *two different momentum regimes* originates from the strong interactions between  ${}^4\text{He}$  atoms. It is this salient feature which is at the heart of the possible formation of the state of supersolid to be discussed in the following section. At the starting point, we have only *one* complex order parameter  $\psi$ . However, due to this unique feature, it splits into *two* complex order parameters  $\psi_1$  and  $\psi_2$  which represent the two low energy modes at the origin and  $k_r$  respectively. The coupling between the two modes is naturally encoded in the quartic  $u$  term in Eqn.5. Note that despite this splitting, there is only one  $U(1)$  global symmetry  $\psi_1 \rightarrow e^{i\chi} \psi_1, \psi_2 \rightarrow e^{i\chi} \psi_2$ . It also has only one Particle-Hole (PH) symmetry  $\psi_1 \rightarrow \psi_1^*, \psi_2 \rightarrow \psi_2^*$ . In principle, the P-H symmetry breaking terms like  $\psi^\dagger \partial_\tau \psi$  may exist, but they are irrelevant in the SF phase. In conventional cases, "hard" spin model is equivalent to "soft" spin model in the long wavelength limit. However, in the presence of the low energy mode  $\psi_2$  at a *finite* roton wavevector  $k = k_r$ , the two models may not be equivalent anymore. Our "soft" spin model Eqn.5 puts the fluctuations of  $\psi_1$  and  $\psi_2$  on the same footing, therefore has the advantage over a "hard" spin model where there is only phase fluctuations.

### III. SUPERFLUID TO SUPERFLUID DENSITY WAVE (SDW) TRANSITION IN THE $\psi$ SECTOR

In this section, neglecting the coupling between the  $n$  sector and the  $\psi$  sector in Eqn.3, we apply the results on the superfluid to superfluid density wave transition in  $\psi$  sector achieved in detail in<sup>20</sup> specifically to  ${}^4\text{He}$  superfluid. In section V, restoring the coupling, we will study the SF to SS transition in the complete QGL action Eqns.1,5,3.

In the superfluid state,  $t < 0$ ,  $\Delta_r > 0$ , so  $\psi_1$  develops a non-vanishing expectation value  $\langle \psi_1 \rangle = a \neq 0$ . As one increases the pressure  $p$ , the interaction  $u$  also gets bigger and bigger, the roton minimum gets deeper and deeper,  $\Delta_r$  gets smaller and smaller as demonstrated by inelastic neutron scattering of superfluid  ${}^4\text{He}$ <sup>21,22</sup>. At mean field level treatment of  $\psi_1$ , simply setting  $\psi_1(\vec{x}, \tau) = a^{25}$  into the interaction term in Eqn.5, we find the interaction term becomes:

$$V(\psi_1 = a, \psi_2) = u[a^4 + |\psi_2|^4 + 2a^2|\psi_2|^2 + 4a^2(\text{Re}\psi_2)^2 + 4a^3\text{Re}\psi_2 + 4a|\psi_2|^2\text{Re}\psi_2] \quad (6)$$

Obviously, the condensation of  $\psi_1$  breaks the  $U(1)$  symmetry of  $\psi_2$ . This is expected, as stressed previously, there is only one  $U(1)$  symmetry anyway. The linear term in  $\psi_2$  in Eqn.6 vanishes, because  $\int d^d x \text{Re}\psi_2(\vec{x}, \tau) = \text{Re}\psi_2(\vec{k} = 0, \tau) = 0$ . Because the  $U(1)$  symmetry of  $\psi_2$  is already broken, it is convenient to separate  $\psi_2$  into real and imaginary parts  $\psi_2(\vec{x}, \tau) = \phi_1(\vec{x}, \tau) + i\phi_2(\vec{x}, \tau)$ , the action inside the SF state is:

$$\begin{aligned} \mathcal{S}_{sf} &= \frac{1}{2} \int_{\Lambda} \frac{d^d k}{(2\pi)^d} \frac{1}{\beta} \sum_{i\omega_n} (\kappa\omega_n^2 + (\Delta_r + 6ua^2) + v_r(k - k_r)^2) |\phi_1|^2 \\ &+ \frac{1}{2} \int_{\Lambda} \frac{d^d k}{(2\pi)^d} \frac{1}{\beta} \sum_{i\omega_n} (\kappa\omega_n^2 + (\Delta_r + 2ua^2) + v_r(k - k_r)^2) |\phi_2|^2 \\ &+ u \int d^d x \int d\tau [(\phi_1^2 + \phi_2^2)^2 + 4a\phi_1^3 + 4a\phi_1\phi_2^2] \end{aligned} \quad (7)$$

Because the particle-hole ( P-H ) symmetry  $\psi_2 \rightarrow \psi_2^*$  remains unbroken, the  $Z_2$  symmetry  $\phi_2 \rightarrow -\phi_2$  remains. Obviously,  $\phi_1$  is more massive than  $\phi_2$ , therefore can be integrated out. Finally, we reach the following  $n = 1$  component ( $d, d_{\perp}$ ) = ( $d + 1, d$ ) quantum Lifshitz (QLF) action<sup>26</sup> to describe superfluid to the superfluid density wave ( SDW ) transition:

$$\begin{aligned} \mathcal{S}_{sf} &= \frac{1}{2} \int_{\Lambda} \frac{d^d k}{(2\pi)^d} \frac{1}{\beta} \sum_{i\omega_n} (\kappa\omega_n^2 + \Delta_{2r} + v_r(k - k_r)^2) |\phi_2|^2 \\ &+ u \int d^d x d\tau \phi_2^4 + \dots \end{aligned} \quad (8)$$

where  $u > 0$ ,  $\Delta_{2r} \sim p_{c1} - p$  is the renormalized mass,  $p_{c1} \sim 25 \text{ bar}$  is the critical pressure of the SF to the SDW transition,  $\dots$  stands for possible high power terms like  $u_{2m}\phi_2^{2m}$ ,  $m \geq 3$ . Note that there is no 3rd power terms like  $\phi_2^3$  due to the  $Z_2$  symmetry of  $\phi_2$ . When

$\Delta_{2r} > 0$ ,  $\langle \psi_2 \rangle = 0$ , the system is in the SF phase. When  $\Delta_{2r} < 0$ , it is in a superfluid density wave phase where  $\langle \psi_2 \rangle$  takes a lattice structure  $\langle \psi_2(\vec{x}) \rangle = e^{i\theta_2} \sum_{m=1}^P \Delta_m e^{i\vec{Q}_m \cdot \vec{x}}$  where  $\theta_2$  is a uniform global phase and  $\vec{Q}_m \sim k_r$ ,  $m = 1, \dots, P^{28}$ . The lattice structure with lattice constant  $a \sim 1/k_r$  can be determined by a energy minimization which depends on microscopic details. Because  $u > 0$ , at mean field level, there is a 2nd order SF to SDW transition at  $\Delta_{2r} = 0$ . This is in sharp contrast to the conventional liquid-solid transition described by Eqn.1 which is first-order transition even at the mean field level due to the presence of a 3rd power term. In<sup>29</sup>, Shankar developed a Renormalization Group ( RG ) analysis to study the stability of Fermi surface under the interactions between fermions. In this RG, the scalings are performed around the Fermi surface where there are low energy excitations. Because there are low energy excitations around the roton surface, it is tempting to apply Shankar's method to study the effects of fluctuations around the roton surface. For simplicity, we only consider classical phase transitions at finite  $T$ , so we set  $\omega_n = 0$  in Eqn.8. Making shift  $k - k_r \rightarrow k$  in the QLF action Eqn.8, we can rewrite the action Eqn 8 as:

$$\begin{aligned} \mathcal{S}_{sf} &= \frac{1}{2} \int_{-\Lambda}^{\Lambda} \frac{dk}{2\pi} \int d\Omega (\Delta_{2r} + v_r k^2) |\phi_2(k, \Omega)|^2 \\ &+ u \left[ \prod_{i=1}^3 \int_{-\Lambda}^{\Lambda} \frac{dk_i}{2\pi} \int d\Omega_i \phi_2(k_1, \Omega_1) \phi_2(k_2, \Omega_2) \right. \\ &\times \left. \phi_2(k_3, \Omega_3) \phi_2(k_4, \Omega_4) + \dots \right] \end{aligned} \quad (9)$$

where momenta conservation is assumed in the interaction  $u$  term and  $\Omega$  is the solid angle in  $d$  dimension. Following Shankar, we integrate out the high energy modes with  $|k| > \Lambda/b$ , keep the low energy modes at  $|k| < \Lambda/b$ . Then rescale  $k' = bk$  and normalize the  $\phi_2$  field such that to keep the  $v_r$  term invariant. We find the recursion relations  $\Delta'_{2r} = b^2 \Delta_{2r}$ ,  $u' = b^3 u$ . In fact,  $u'_{2m} = b^{m+1} u_{2m}$  for any  $m$ . So all the possible interaction terms are relevant. It indicates that the SF-SDW transition is always fluctuation driven first order. This RG analysis confirms the original picture in<sup>30</sup>. This is in sharp contrast to the interacting fermions where only the quartic term  $u$  is marginally relevant ( irrelevant ) if it is positive ( negative ), while high power terms like  $u^{2m}$ ,  $m \geq 3$  are irrelevant.

### IV. SUPERFLUID TO NORMAL SOLID TRANSITION

In the last section, we studied the SF to SDW transition in the  $\psi$  sector. In this section, we will study the SF to the NS transition. In the superfluid state, if the multi-quasiparticle part can be neglected in the dynamic structure factor, the Feymann relation between the Landau quasi-particle dispersion relation in the  $\psi$  sector and

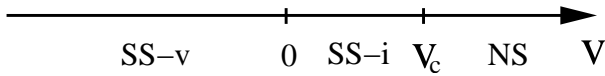


FIG. 1: There possible zero temperature phases when  $p_{c1} < p < p_{c2}$  ( See the vertical axis in Fig.3) depending on the sign and strength of the coupling in Eqn.3. When  $v < 0$ , the SS is vacancy induced ( SS-v ). When  $0 < v < v_c$ , the SS is interstitial induced ( SS-i ). When  $v > v_c$ , there can only be NS. The SF to NS transition is studied in this section. The SS to SS-v and SS-i transitions will be studied in the next section.

the static structure factor in the  $n$  sector holds:

$$\omega(q) = \frac{q^2}{2mS(q)} \quad (10)$$

In the  $q \rightarrow 0$  limit,  $S(q) \sim q$ ,  $\omega(q) \sim q$  recovers the superfluid phonon spectrum near  $q = 0$  in the  $\psi_1$  sector. The first maximum peak in  $S(q)$  corresponds to the roton minimum in  $\omega(q)$  in the  $\psi_2$  sector ( Fig.2b ), namely,  $k_n = k_r$ . As one increases the pressure  $p$ , the interaction  $u$  also gets bigger and bigger, the first maximum peak of  $S(q)$  increases, the roton minimum  $\Delta_r$  gets smaller and smaller<sup>21</sup>. Across the critical pressure  $p = p_c$ , there are the two possibilities. (1) The resulting solid is a commensurate solid, then  $\langle \psi \rangle = 0$ . There is no remanent of the SF in the NS, the supersolid phase does not exist as an equilibrium ground state. This is the SF to NS transition. As shown in section VI, this happens when  $v_i$  is larger than some critical values  $v > v_c$  ( Fig.2 ). (2) In the next section, we will discuss the second case  $v < v_c$  which is the SF to the SS transition ( Fig.3).

The effective action inside the SF is :

$$\mathcal{L}[\delta n, \theta] = i\delta n \partial_\tau \theta + \frac{1}{2}\rho_s(\nabla\theta)^2 + \frac{1}{2}\delta n V_n(\vec{q})\delta n \quad (11)$$

where  $\rho_s$  is the superfluid density and  $V_n(q) = a - bq^2 + cq^4$  with  $a > 0, b > 0$  is the density-density interaction between the  ${}^4\text{He}$  atoms.

In the SF state, it is convenient to integrate out  $\delta n$  in favor of the phase field  $\theta$  to get the phase representation

$$\mathcal{L}[\theta] = \frac{1}{2V_n(\vec{q})}(\partial_\tau\theta)^2 + \frac{1}{2}\rho_s(\nabla\theta)^2 \quad (12)$$

where the dispersion relation of the superfluid modes including higher orders of momentum can be extracted:

$$\omega^2 = [\rho_s V_n(\vec{q})]q^2 = 2\rho_s q^2(a - bq^2 + cq^4) \quad (13)$$

It is easy to see that the dispersion relation indeed has the form shown in Fig.2b with a roton minimum. Because the original instability comes from the density-density interaction  $V_n(\vec{q})$ , it is convenient to integrate out the phase field in favor of the density fluctuation operator  $\delta n$ . Neglecting the vortex excitations in  $\theta$  and

integrating out the  $\theta$  in Eqn.11 leads to:

$$\mathcal{L}[\delta n] = \frac{1}{2}\delta n(-\vec{q}, -\omega_n)\left[\frac{\omega_n^2}{\rho_s q^2} + V_n(\vec{q})\right]\delta n(\vec{q}, \omega_n) \quad (14)$$

where we can identify the dynamic pseudo-spin density-density correlation function  $S_n(\vec{q}, \omega_n) = \langle \delta n(-\vec{q}, -\omega_n)\delta n(\vec{q}, \omega_n) \rangle = \frac{\rho_s q^2}{\omega_n^2 + v^2(q)q^2}$  where  $v^2(q) = \rho_s V_n(q)$  is the spin wave velocity.

From the pole of the dynamic density-density correlation function, we can identify the speed of sound wave which is exactly the same as the spin wave velocity. This should be expected. From the analytical continuation  $i\omega_n \rightarrow \omega + i\delta$ , we can identify the dynamic structure factor:  $S_n(\vec{q}, \omega) = S_n(q)\delta(\omega - v(q)q)$  where  $S_n(q) = \rho_s q\pi/2v(q)$  is the equal time density correlation function shown in Fig.2b. As  $q \rightarrow 0$ ,  $S_n(q) \rightarrow q$ . The *Feymann relation* which relates the dispersion relation to the equal time structure factor is:

$$\omega(q) = \frac{\rho_s \pi q^2}{2S_n(q)} \quad (15)$$

which takes exactly the same form as Eqn.10 if we identify  $\rho_s \sim 1/m$  with  $m$  the mass of  ${}^4\text{He}$  mass. Therefore, we recovered the Feymann relation from our GL theory Eqn.11 which gives us the confidence that Eqn.11 is the correct starting action to study the the SF to SS transition. The density representation Eqn.14 is *dual* to the phase representation Eqn.12. However, the phase representation Eqn.12 contains explicitly the superfluid order parameter  $\psi \sim e^{i\theta}$  which can be used to characterize the superfluid order in the SF phase. While in Eqn.14, the signature of the superfluid phonon mode is encoded in the density sound mode, because the order parameter  $\psi$  is integrated out, the superfluid order is hidden, so it is not as powerful as the phase representation in describing the SF state. However, as shown in the following, when describing the transition from the ES to the NS, the density representation Eqn.14 has a big advantage over the phase representation.

Because the instability is happening at  $q = q_0$  instead of at  $q = 0$ , the vortex excitations in  $\theta$  remain *uncritical* through the SF to SS transition. Integrating them out will generate interactions among the density  $\delta n$ :

$$\begin{aligned} \mathcal{L}[\delta n] &= \frac{1}{2}\delta n(-\vec{q}, -\omega_n)\left[\frac{\omega_n^2}{\rho_s q^2} + V_n(\vec{q})\right]\delta n(\vec{q}, \omega_n) \\ &- w(\delta n)^3 + u(\delta n)^4 + \dots \end{aligned} \quad (16)$$

where the momentum and frequency conservation in the quartic term is assumed. Note that the  $(\omega_n/q)^2$  term in the first term stands for the quantum fluctuations of  $\delta n$  which is absent in the classical NL to NS transition Eqn.1. Because of the lack of  $Z_2$  exchange symmetry, there is a cubic term in Eqn.17. Expanding  $V_n(q)$  near the roton minimum  $q_0$  leads to the quantum Ginsburg-

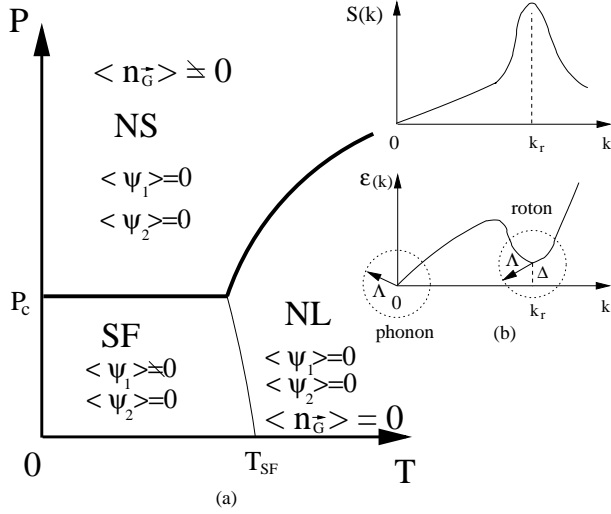


FIG. 2: (a) The theoretical phase diagram of GL model Eqns.1,2 and 5 in  $-\Delta_r \sim p - p_{c1}$  versus  $t \sim T - T_c$  plane. This happens when the repulsive coupling  $v_i$  in Eqn.3 is larger than a critical value  $v > v_c$  ( Fig.1) .  $T$  controls thermal fluctuations, while  $p$  tunes quantum fluctuations. SF is the superfluid phase, NS is the normal solid phase, NL is the normal liquid phase. The supersolid phase is absent. Thick ( thin ) lines are 1st ( 2nd ) order transitions. The critical temperatures  $T_{SF}$  of NL to SF transition drops slightly as the pressure  $p$  increases because of the quantum fluctuations. The SF to NS transition is described by the QGL Eqn.17. (b) The structure factor and the separation of low ( phonon ) and high ( roton ) momenta regime in the dispersion relation in the SF. The Feynmann relation between the two curves are explicitly derived in the text

Landau action to describe the SF to the NS transition:

$$\begin{aligned} \mathcal{L}[\delta n] = & \frac{1}{2} \delta n [A_n \omega_n^2 + r + c(q^2 - q_0^2)^2] \delta n \\ & - w(\delta n)^3 + u(\delta n)^4 + \dots \end{aligned} \quad (17)$$

where  $r \sim p_{c1} - p$  and  $A_\rho \sim \frac{1}{\rho_s q_0^2}$  which is non-critical across the transition. The generic transition driven by the collapsing of roton minimum is from SF to NS instead of from the SF to the supersolid ( SS ). In the SF,  $r > 0$ ,  $\langle \psi \rangle \neq 0$ ,  $\langle \delta n \rangle = 0$ , In the NS,  $r < 0$ ,  $\langle \psi \rangle = 0$ ,  $\langle \delta n \rangle = \sum'_{\vec{G}} n_{\vec{G}} e^{i\vec{G} \cdot \vec{x}}$  where  $\vec{G}$  are the shortest reciprocal lattice vector of the resulting lattice.

The corresponding phase diagram for the SF to the NS transition is:

In the Fig.2, even the SS does not exist as an equilibrium state, it may still exist as a metastable state which is interesting on its own, because it may have important observable effects which will be discussed in Section IX. A similar 2 + 1 dimensional zero temperature excitonic superfluid to pseudo-spin density wave (PSDW) transition in bilayer quantum Hall system was worked out in<sup>50</sup>.

## V. SUPERFLUID TO SUPERSOLID TRANSITION AND GLOBAL PHASE DIAGRAM

In the last two sections, we discuss the SF to the SDW transition with the order parameter  $\psi$  and the SF to the NS transition with the order parameter  $\delta n$  respectively. In this section, we discuss the SF to the SS transition with both order parameters  $\psi$  and  $\delta n$ . Then we have to also include the coupling between  $n$  and  $\psi$  sector encoded in Eqn.3. As pointed out in<sup>20</sup>, the most difficult uncertainty in the SF-SDW transition is to determine the lattice structure of the SDW in the  $\psi$  sector which depends on microscopic details. Very fortunately, as shown in this section, this uncertainty disappears when the coupling Eqn.3 is taken into account, the SF to SDW transition in the  $\psi$  sector becomes a SF to SS transition in the <sup>4</sup>He system.

Across the phase boundary  $p = p_{c1}$  in Fig.2, the resulting solid could be an in-commensurate solid ( IC-NS ) with vacancies or interstitials even at  $T = 0$  whose condensation leads to  $\langle \psi \rangle \neq 0$ <sup>2,3,15</sup>. There is still some remnant of the SF in the IC-NS, the supersolid phase does exist as an equilibrium ground state. As shown in the next section, for vacancies, there is no constraints on  $v_i$ . However, for interstitials, this happens when  $v_i$  is smaller than some critical values  $v_i < v_{ic}$ , then a SS-state has a lower energy than a NS state at sufficiently low temperature ( Fig.1). In the GL theory,  $v_i$  is used as an input parameter, so it is difficult to determine which case will happen. In this section, we assume  $v_i < v_{ic}$  and study the SF to the SS transition across  $p = p_{c1}$ . Because  $\psi$  is *also critical* through the transition, we can not simply integrate it out like in the last section. In fact, in the effective GL theory, we have to treat  $n$  and  $\psi$  on the same footing. From Eqn.1 and Eqn.5, we can see that  $n$  and  $\psi_2$  have very similar propagators, so the lattice formation in  $n$  sector with  $n(x) = n_0 + \sum'_{\vec{G}} n_{\vec{G}} e^{i\vec{G} \cdot \vec{x}}$  where  $G = k_n$  and the superfluid density wave ( SDW ) formation in  $\psi_2$  sector with  $\langle \psi_2(\vec{x}) \rangle = e^{i\theta_2} \sum_{m=1}^P \Delta_m e^{i\vec{Q}_m \cdot \vec{x}}$  where  $Q_m = k_r = k_n \sim 2\pi/a \sim 2\pi/3.17\text{\AA}$  have to happen simultaneously. From Hansen-Verlet criterion<sup>26</sup>, when  $S(k_n)/n_0$  is sufficiently large, solidification in the  $n$  sector occurs, so the roton minimum remains *finite* just before its condensation. So strictly speaking, the RG analysis in Eqn.9 holds only in the absence of the  $n - \psi$  coupling. The SDW  $\rho = |\psi_1 + \psi_2|^2$  is simply locked to ( or commensurate with ) the underlying normal solid (  $n$  ) lattice. In fact, this locking is dictated by the  $\rho$  density- $n$  density coupling in Eqn.3. If the coupling is attractive  $v_v > 0$ , the SDW just coincides with the  $n$  lattice. If it is repulsive  $v_i > 0$ , then it simply shifts the SDW by suitable constants along the three unit vectors in the direct lattice. These constants will be determined in the next section for different  $n$  lattices. Namely, the supersolid states consist of two inter-penetrating lattices formed by the  $n$  lattice and the  $\psi_2$  superfluid density wave. In fact, in a carefully prepared super-pressured sample, the roton

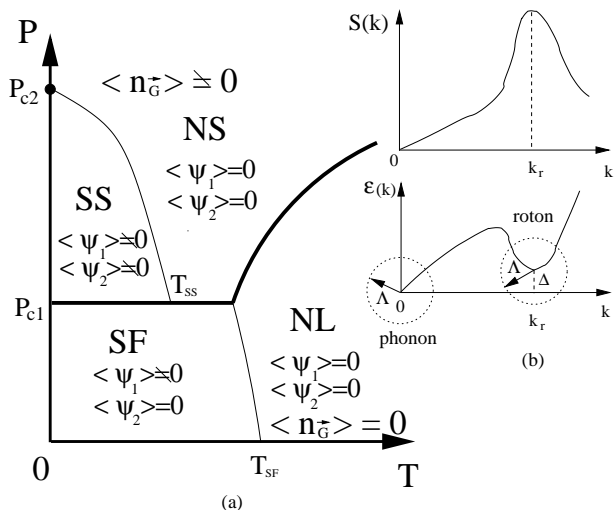


FIG. 3: (a) The theoretical phase diagram of GL model Eqns.1,2 and 5 in  $-\Delta_r \sim p - p_{c1}$  versus  $t \sim T - T_c$  plane.  $T$  controls thermal fluctuations, while  $p$  tunes quantum fluctuations. SF is the superfluid phase, NS is the normal solid phase, NL is the normal liquid phase. The SS is either vacancies induced supersolid (SS-v) or interstitials induced supersolid (SS-i) phase. For SS-i, this happens only when the repulsive coupling  $v_i$  in Eqn.3 is smaller than a critical value  $v_i < v_{ic}$  (Fig.1). Thick (thin) lines are 1st (2nd) order transitions. The critical temperatures of NL to SF and NS to SS transitions drop slightly as the pressure  $p$  increases because of the quantum fluctuations. The SF to the SS transition is a simultaneous combination of the SDW transition in  $\psi$  sector driven by the roton condensation at  $k_0 = k_r$  and the NS transition in the  $n$  sector driven by the divergence of the structure function at  $k_0 = k_r = k_n$ . (b) The structure factor and the separation of low (phonon) and high (roton) momenta regime in the SF.

minimum survives up to as high pressure as  $p_r \sim 120$  bar. This fact suggests the roton minimum in the meta-stable state in a super-pressured sample is replaced by a SDW which is commensurate with the  $n$  lattice in the stable SS state. Strikingly, this pressure  $p_r \sim 120$  bar is close to  $p_{c2} \sim 170$  bar in Fig.3 where the NCRI was extrapolated to vanish in the PSU's experiments<sup>10</sup>. This consistency also lead some support to the above picture. Obviously, when the pressure is so high that  $p > p_{c2}$  in Fig.3, C-NS is the only possible ground state, any remanent of the SF completely disappears. So the vertical axis in the Fig.3 shows the SF-SS-NS series as the pressure  $P$  increases at  $T = 0$

Combining the roton condensation picture<sup>31</sup> in the last section with the results reviewed in the introduction, we can sketch the following phase diagram Fig.3 of the complete QGL Eqns 1, 5 and 3.

As can be seen from the Fig.3, starting from the SF side, as the pressure is increased at a given temperature, there are two possible states (1) At very low  $T < T_{SS}$ , the Bose-Einstein condensation (BEC) of  $\psi_2$  leads to the su-

persolid state where  $\langle \psi_1 \rangle \neq 0, \langle \psi_2 \rangle \neq 0, \langle n_{\vec{G}} \rangle \neq 0$ . The instability happens at a finite wavevector  $k = k_r$  instead of at  $k = 0$ . (2) At higher temperature  $T_{SS} < T < T_{SF}$ , there is a direct SF to NS transition. The SS state is certainly different from a conventional normal solid phase where  $\langle \psi_1 \rangle = \langle \psi_2 \rangle = 0, \langle n_{\vec{G}} \rangle \neq 0$ . In addition to the conventional translational and rotational orders characterized by  $\rho$  (which is the same as those characterized by  $n$ ), the SS also has the ODLRO characterized by  $\psi_1$  and  $\psi_2$ . When decreasing the temperature at a given pressure, if  $p < p_c$ , the NL becomes SF at  $T = T_{SF}$ , the instability happens at  $k = 0$ . If  $p > p_c$ , the NL becomes a NS first at  $T = T_m$ , then there is a SDW onset transition from the NS to a SS phase at  $T = T_{SS}$ . Starting from  $T = 0$  and increasing the temperature, if  $p < p_c$ , the transition from the SF to the NL is driven by vortex unbindings; if  $p > p_c$ , the transition from the SS to the NS is also driven by the vortex unbinding in the global phase  $\theta_2$  (see Eqn.21), the phonon modes in the SS are non-critical across the transition, as the temperature increases further, the phonon modes drive the melting of the NS into the NL.

Because the SF to SS transition driven by the roton condensation can be either weakly or strong first order, in principle, Eqns.8,17 work precisely only in the SF side, it is not easy to study the precise nature of the SS state from the SF side. It turns out that it is more convenient to study the properties of the SS state from the NS side in the following section. The results achieved from the NS side in the following section indeed confirm the roton condensation picture and the global phase diagram Fig. 1.

## VI. THE NORMAL SOLID TO THE SUPERSOLID TRANSITION

In this section, we approach the SS phase from the normal solid side and confirm it indeed exists and determine its lattice structure. In the NL, the BEC happens in the  $\psi_1$  sector at  $k = 0$ ,  $\psi_2$  has a large gap and can be simply integrated out. In the NS,  $\psi$  stands for the vacancies or interstitials coming from the large zero point quantum fluctuations<sup>2,3,15</sup>. In the following, we discuss SS-v and SS-i respectively.

### A. Vacancies induced supersolid: SS-v

The resulting solid could be an in-commensurate solid with vacancies even at  $T = 0$  whose condensation leads to  $\langle \psi \rangle \neq 0$ . The SS-v state has a lower energy than a NS state at sufficiently low temperature. Inside the NS, the translational symmetry is already broken, we can simply set  $n(\vec{x}) = n_0 + \sum_{\vec{G}} n_{\vec{G}} e^{i\vec{G} \cdot \vec{x}}$  and put it into Eqn.3, then Eqn.2, Eqn.3 has only the symmetry of translation by a lattice constant. In the presence of the periodic potential of  $n(x)$  lattice,  $\psi$  will form a Bloch wave, the  $u$  interaction

of  $\psi$  in Eqn.8 will certainly favor extended Bloch wave over strongly localized Wannier state. In principle, a full energy band calculation incorporating the interaction  $u$  is necessary to get the energy bands of  $\psi$ . Fortunately, qualitatively important physical picture of GL Eqns.1, 5, 3 can be achieved without such a detailed energy band calculation. In the following, substituting the ansatz  $\langle \psi_1(\vec{x}) \rangle = ae^{i\theta_1}$  and  $\langle \psi_2(\vec{x}) \rangle = e^{i\theta_2} \sum_{m=1}^P \Delta_m e^{i\vec{Q}_m \cdot \vec{x}}$  where  $Q_m = Q$  into Eqn.3, we study the effects of  $n$  lattice on  $\psi = \psi_1 + \psi_2$ . From Eqn.3, we can see  $n(x)$  acts as a periodic potential on  $\psi$ . In order to get the lowest energy ground state, we must consider the following 4 conditions: (1) because any complex  $\psi$  ( up to a global phase ) will lead to local supercurrents which is costly, so we can take  $\psi$  to be real, so  $\vec{Q}_m$  have to be paired as anti-nodal points.  $P$  has to be even (2) as shown from the Feymann relation Eqn.10,  $\vec{Q}_m, m = 1, \dots, P$  are simply  $P$  shortest reciprocal lattice vectors, then translational symmetry of the lattice dictates that  $\epsilon(\vec{K} = 0) = \epsilon(\vec{K} = \vec{Q}_m)$ ,  $\psi_1$  and  $\psi_2$  have to condense at the same time<sup>32</sup> (3) The point group symmetry of the lattice dictates  $\Delta_m = \Delta$  and is real (4) for the vacancies case, the interaction is attractive  $v_v < 0$ , the SDW-v simply sits on top of the  $n$  lattice, so the Superfluid Density wave  $\rho = |\psi|^2$  simple sits on top of the  $n$  lattice as much as possible. This is reasonable, because vacancies are hopping on near the lattice sites, so the Bose condensation of vacancies also happen near the lattice sites. The attractive interaction favors  $\psi(x = \vec{R}/2) \sim 0$  where  $\vec{R}/2$  stands for any interstitial sites which are in the middle of lattice points. It turns out that the the 4 conditions can fix the relative phase and magnitude of  $\psi_1$  and  $\psi_2$  to be  $\theta_2 = \theta_1 + \pi, \Delta = a/P$ , namely:

$$\psi_{ssv} = \psi_0 \left( 1 + \frac{2}{P} \sum_{m=1}^{P/2} \cos \vec{Q}_m \cdot \vec{x} \right) \quad (18)$$

where  $\psi_0 = ae^{i\theta}$  depends on the temperature and pressure. Note that in contrast to a uniform superfluid, the magnitude of  $\psi$  is changing in space. This field satisfies the Bloch theorem with the crystal momentum  $\vec{k} = 0$  and the Fourier components are  $\psi(\vec{K} = 0) = a, \psi(\vec{K} = \vec{Q}_m) = a/P$ . They have the same sign and decay in magnitude. In principle, higher Fourier components may also exist, but they decay very rapidly, so can be neglected without affecting the physics qualitatively.

### B. Interstitial induced supersolid: SS-i

In the interstitial case, due to the  $n$  lattice formation, the mass of  $\psi_1$  was increased to  $t_{\psi_1}^{NS} = t + v_i^{NS} n_0 = T - T_{SS-i}$ . Subtracting it from  $t_{\psi_1}^{NL} = t + v_i^{NL} n_0 = T - T_{SF}$  leads to  $T_{SF} - T_{SS-i} = n_0 \Delta v_i$ . So the transition temperature  $T_{SS-i}$  from the NS to the SS will *shift down* to lower temperature as shown in Fig.3. Without losing any generality, one can take the NL as the reference

state, namely, set  $v_1^{NL} = 0$ . If  $v_i$  is larger than a critical value  $v_i > v_{ic}$ , then  $T_{SS-i}$  is suppressed to zero ( Fig.1). This is the case discussed in section IV. The SS-i disappears from the phase diagram. The resulting solid is a commensurate solid. In the following, we only focus on  $v_i < v_{ic}$ , so  $T_{SS-i} > 0$ , the SS-i state exists in the Fig.3. The resulting solid could be an in-commensurate solid with interstitials even at  $T = 0$  whose condensation leads to  $\langle \psi \rangle \neq 0$ . The SS state has a lower energy than a NS state at sufficiently low temperature. Then the temperature shift  $\Delta T = T_{SF} - T_{SS-i}$  is an effective experimental measure of the repulsive coupling  $v_i$  in Eqn.3. The rest arguments go the same as in the vacancies case discussed in (A), the only important difference is the condition (4), the interaction is attractive  $v_v < 0$ , the SDW-v simply sits on top of the  $n$  lattice. However, for the interstitials case, the interaction is repulsive  $v_i > 0$  favors  $\psi(x = 0) \sim 0$ , so the Superfluid Density wave  $\rho = |\psi|^2$  can avoid the  $n$  lattice as much as possible. This is reasonable, due to the competing of the the two orders, the superfluid component emerges from the places where the normal solid component is suppressed. It turns out that the the 4 conditions can fix the relative phase and magnitude of  $\psi_1$  and  $\psi_2$  to be  $\theta_2 = \theta_1 + \pi, \Delta = a/P$ , namely:

$$\psi_{ssi} = \psi_0 \left( 1 - \frac{2}{P} \sum_{m=1}^{P/2} \cos \vec{Q}_m \cdot \vec{x} \right) \quad (19)$$

where  $\psi_0 = ae^{i\theta}$  depends on the temperature and pressure. Note that the crucial sign difference from the vacancies case which make an important difference from the X-ray scattering from SS-v and SS-i to be discussed in the next section. Again in contrast to a uniform superfluid, the magnitude of  $\psi$  is changing in space. This field satisfies the Bloch theorem with the crystal momentum  $\vec{k} = 0$  and the Fourier components are  $\psi(\vec{K} = 0) = a, \psi(\vec{K} = \vec{Q}_m) = -a/P$ . They oscillate in sign and decay in magnitude. In principle, higher Fourier components may also exist, but they decay very rapidly, so can be neglected without affecting the physics qualitatively.

In the following, we will discuss different lattice structures of  $n$  when  $P = 2, 4, 6, 8, 12$  respectively. Obviously, the Superfluid Density wave  $\rho = |\psi|^2$  has the same Bravais lattice structure as the the  $n$  lattice. However, as shown in the following, even  $n$  is a Bravais lattice, the SDW may be the same Bravais lattice plus a few basis.

(a) P=2:  $\vec{Q}_1 = -\vec{Q}_2 = \vec{Q}$  are a pair of anti-nodal points. They are the two shortest reciprocal lattice vectors generating a 1 dimensional lattice embedded in a 3 dimensional system. The field is  $\psi(\vec{x}) = a(1 - \cos \vec{Q} \cdot \vec{x})$ . There is a superfluid density wave formation transition inside the normal solid which is a 2nd order transition in the universality class of 3D XY model( Fig.3). The local SDW operator  $\rho_s^l = |\psi(\vec{x})|^2 = a^2(1 - \cos \vec{Q} \cdot \vec{x})^2$ . It breaks translational invariance only along 1-dimension which is similar to Smectic-A or Smectic-C phase in the

liquid crystal<sup>26</sup>. The maxima of the SDW  $\psi_{max} = 2a$  appear exactly in the middle of lattice points at  $\vec{a} = \frac{1}{2}\vec{a}_1$ . So the SDW forms the dual lattice of the 1d lattice which is also a 1d lattice.

(b) P=4:  $\vec{Q}_3 = -\vec{Q}_1, \vec{Q}_4 = -\vec{Q}_2, \vec{Q}_1 \cdot \vec{Q}_2 = 0, \vec{Q}_i, i = 1, 2, 3, 4$  form the 4 corners of a square. They are the four shortest reciprocal lattice vectors generating a 2 dimensional square lattice embedded in a 3 dimensional system. The field is  $\psi(\vec{x}) = a[1 - \frac{1}{2}(\cos \vec{Q}_1 \cdot \vec{x} + \cos \vec{Q}_2 \cdot \vec{x})]$ . The local SDW operator  $\rho_s^l = |\psi(\vec{x})|^2$ . The maxima of the SDW  $\psi_{max} = 2a$  appear exactly in the middle of lattice points at  $\vec{a} = \frac{1}{2}(\vec{a}_1 + \vec{a}_2)$ . So the SDW forms the dual lattice of the square lattice which is also a square lattice.

(c) P=6: there are two cases need to be discussed separately. (c1)  $\vec{Q}_i, i = 1, 2, 3, 4, 5, 6$  form the 6 corners of a hexagon. They consist of the 6 shortest reciprocal lattice vectors generating a 2 dimensional triangular lattice embedded in a 3 dimensional system. The field is  $\psi(\vec{x}) = a[1 - \frac{1}{3}(\cos \vec{Q}_1 \cdot \vec{x} + \cos \vec{Q}_2 \cdot \vec{x} + \cos \vec{Q}_3 \cdot \vec{x})]$ . The maxima of the SDW  $\psi_{max} = 3/2a$  appear in the middle of lattice points at  $\vec{a} = \pm \frac{1}{3}(\vec{a}_1 + \vec{a}_2)$ . They form the dual lattice of the triangular lattice which is a honeycomb lattice. The honeycomb lattice is not a Bravais lattice which has two triangular sublattices  $A$  and  $B$ , it can be considered as one triangular lattice  $A$  plus a basis. This can be understood intuitively: there are two equivalent ways to shift the  $n$  lattice, one way to get the sublattice  $A$ , the other to get the sublattice  $B$ . Putting  $A$  and  $B$  together forms the SDW which takes the honeycomb lattice (c2)  $\vec{Q}_i, i = 1, 2, 3, 4, 5, 6$  are the 6 shortest reciprocal lattice vectors generating a cubic lattice. The maxima of the SDW  $\psi_{max} = 2a$  appear exactly in the middle of lattice points at the 8 points  $\vec{a} = \frac{1}{2}(\pm \vec{a}_1 \pm \vec{a}_2 \pm \vec{a}_3)$ . So the SDW forms the dual lattice of the cubic lattice which is also a cubic lattice.

(d)  $P = 8$ :  $\vec{Q}_i, i = 1, \dots, 8$  form the 8 shortest reciprocal lattice vectors generating a  $bcc$  reciprocal lattice which corresponds to a  $fcc$  direct lattice. The field is  $\psi(\vec{x}) = a[1 - \frac{1}{4}(\cos \vec{Q}_1 \cdot \vec{x} + \cos \vec{Q}_2 \cdot \vec{x} + \cos \vec{Q}_3 \cdot \vec{x} + \cos \vec{Q}_4 \cdot \vec{x})]$ . The maxima of the SDW  $\psi_{max} = 2a$  appear in all the edge centers such as  $(1/2, 0, 0)$  etc. and the centers of any cube such as  $(1/2, 1/2, 1/2)$  etc. It is easy to see these points can be achieved by simply shifting the  $n$  lattice by  $(1/2, 1/2, 1/2)$ , so the SDW also forms a  $fcc$  direct lattice.

(e)  $P = 12$ :  $\vec{Q}_i, i = 1, \dots, 12$  form the 12 shortest reciprocal lattice vectors generating a  $fcc$  reciprocal lattice which corresponds to a  $bcc$  direct lattice. The field is  $\psi(\vec{x}) = a[1 - \frac{1}{6}(\cos \vec{Q}_1 \cdot \vec{x} + \cos \vec{Q}_2 \cdot \vec{x} + \cos \vec{Q}_3 \cdot \vec{x} + \cos \vec{Q}_4 \cdot \vec{x} + \cos \vec{Q}_5 \cdot \vec{x} + \cos \vec{Q}_6 \cdot \vec{x})]$ . The maxima of the SDW  $\psi_{max} = 4/3a$  appear along any square surrounding the center of the cube such as  $(1/2, \beta, 0)$  or  $(1/2, 0, \gamma)$  etc. In fact, one can achieve the SDW lattice by shifting the center of  $bcc$  to the 3 face centers, so all these points are on the edge centers and face centers which are only discrete points on the square surrounding the center of the cube. We expect the continuous whole square is due to

the artifact of the approximation  $\psi(x=0) \sim 0$  imposed. So the SDW  ${}^4He$  in Vycor glass takes a  $bcc$  lattice.

Unfortunately, a spherical  $k = Q$  surface can not lead to lattices with different lengths of primitive reciprocal lattice vectors such as a  $hcp$  lattice. This is similar to the classical liquid-solid transition described by Eqn.1 where a single maximum peak in the static structure factor can not lead to a  $hcp$  lattice<sup>26</sup>. Another difficulty with the  $hcp$  lattice is that the  $hcp$  lattice is not a Bravais lattice, it consist of two inter-penetrating simple hexagonal lattices shifted by  $\vec{a} = \frac{1}{3}\vec{a}_1 + \frac{1}{3}\vec{a}_2 + \frac{1}{2}\vec{a}_3$ . Here we can simply take the experimental fact that  $n$  forms a  $hcp$  lattice without knowing how to produce such a lattice from a GL theory Eqn.1. Despite the technical difficulty, because for an idea  $hcp$  lattice  $c/a = \sqrt{8/3}$ , an  $hcp$  lattice has 12 nearest neighbors, so its local environment may resemble that of an  $fcc$  lattice. We expect the physics ( except the anisotropy of NCRI in the  $hcp$  lattice to be discussed in the next two sections ) is qualitatively the same as that in  $fcc$  direct lattice. From the insights achieved from the other lattices, one can achieve the SDW lattice by shifting the  $hcp$  lattice of  $n$  by  $\vec{a} = \frac{2}{3}(\vec{a}_1 + \vec{a}_2) + \frac{1}{4}\vec{a}_3$ .

### C. Discussions on both SS-v and SS-i

In fact, for both SS-v and SS-i, we can write  $n$  and  $\psi$  sector in a more symmetric way:  $n(\vec{x}) = n_0 + \sum_{\vec{G}} n_{\vec{G}} e^{i\vec{G} \cdot \vec{x}}, \psi(\vec{x}) = \psi_0 + \sum_{\vec{G}} \psi_{\vec{G}} e^{i\vec{G} \cdot \vec{x}}$ . It is easy to see that in the SS, the translational symmetry  $\vec{x} \rightarrow \vec{x} + \vec{a}, n_{\vec{G}} \rightarrow n_{\vec{G}} e^{i\vec{G} \cdot \vec{a}}, \psi_{\vec{G}} \rightarrow \psi_{\vec{G}} e^{i\vec{G} \cdot \vec{a}}$  is broken down to  $\vec{a} = \vec{R}, n_{\vec{G}} \rightarrow n_{\vec{G}} e^{i\vec{G} \cdot \vec{R}} = n_{\vec{G}}, \psi_{\vec{G}} \rightarrow \psi_{\vec{G}} e^{i\vec{G} \cdot \vec{R}} = \psi_{\vec{G}}$ . In the Fig.3, in the NL side, as the temperature is lowered, the symmetry breaking happens in  $\psi_1$  at  $k = 0$ , the NL gets into the SF. However, as shown in this section, in the NS side, the symmetry breaking happens in both the  $\psi_1$  at  $k = 0$  and  $\psi_2$  sector at  $P$  discrete points in a spherical surface  $k = Q$  simultaneously, the NS gets to the SS state at a much lower critical temperature  $T_{SS}$ . The results achieved from the NS side in this section indeed confirm Fig.3 achieved from the roton condensation picture in the SF phase in the last section.

## VII. EXCITATIONS IN THE SUPERSOLID

So far, we only look at the mean field solutions corresponding to vacancies and interstitials. Here we discuss excitations above the mean field solutions. It turns out that the excitations in both cases are the same, so we discuss both cases at same time. In the SS-v and SS-i, the wavefunctions can be written as

$$\psi_{ss} = \psi_0 (1 \pm \frac{2}{P} \sum_{m=1}^{P/2} \cos \vec{Q}_m \cdot \vec{x}), \quad \psi_0 = |\psi_0| e^{i\theta} \quad (20)$$

where  $\pm$  sign corresponds to SS-v and SS-i respectively. Obviously, there are also topological defects in the phase

winding of  $\theta$  which are vortices. At  $T \ll T_{SS}$ , the vortices can only appear in tightly bound pairs. However, as  $T \rightarrow T_{SS}^-$ , the vortices start to become liberated, this process renders the total NCRI to vanish above  $T > T_{SS}$ . In addition to the superfluid  $\theta$  mode in SS states, there are also lattice phonon modes  $\vec{u}$  in both  $n$  sector and  $\psi_2$  sector. However, it is easy to see that the coupling Eqn.3 is invariant under  $\vec{x} \rightarrow \vec{x} + \vec{u}$ ,  $n(\vec{G}) \rightarrow n(\vec{G})e^{i\vec{G}\cdot\vec{u}}$ ,  $\psi(\vec{G}) \rightarrow \psi(\vec{G})e^{i\vec{G}\cdot\vec{u}}$ , so the lattice phonon modes in  $\psi$  are locked to those in the conventional  $n$  lattice<sup>34</sup>. This is expected because there is only one kind of translational symmetry breaking, therefore only one kind of lattice phonons. The coupling between the  $\theta$  mode and the  $\vec{u}$  mode was worked out in<sup>27</sup>. *If ignoring the coupling between the superfluid  $\theta$  mode and the phonon  $\vec{u}$  mode*, then the action to describe the NS to SS transition in a static lattice is:

$$f_{\psi_0} = K_{NS}|\nabla\psi_0|^2 + t_{NS}|\psi_0|^2 + u_{NS}|\psi_0|^4 + \dots \quad (21)$$

where  $t_{NS} = T - T_{SS}$ . Note that this equation works for both SS-v and SS-i. Obviously, it is still a 3d XY transition. It was shown in<sup>14</sup> that the coupling to the phonon mode  $\vec{u}$  will not change the universality class. A low energy effective action involving the superfluid phonon  $\theta$ , the lattice phonons  $\vec{u}$  and their couplings will be discussed in<sup>27</sup>.

In the SF phase, a single vortex costs a lot of energy  $E_v^{SF} = \frac{\rho_s^{SF} h^2}{4\pi m^2} \ln \frac{R}{\xi_{SF}}$  where  $m$  is the mass of He atom,  $R$  is the system size and  $\xi_{SF} \sim a$  is the core size of the vortex. This energy determines the critical velocity in SF  $v_c^{SF} > 30 \text{ cm/s}$ . Because the long distance behavior of SS is more or less the same as SF, we can estimate its single vortex energy  $E_v^{SS} = \frac{\rho_s^{SS} h^2}{4\pi m^2} \ln \frac{R}{\xi_{SS}}$  where  $\rho_s^{SS}$  is the *global* superfluid density inside the SS. We expect the core size of a supersolid vortex  $\xi_{SS} \sim 1/\Lambda \gg 1/k_r \sim a \sim \xi_{SF}$ . So inside the SS vortex core, we should also see the lattice structure of  $n$ <sup>37</sup>. This is similar to the phenomenon that DW ordered states were detected in the vortex core of high temperature superconductors<sup>35,36</sup>. In fact, because  $\psi(x)$  stands for vacancies or interstitials, we expect that  $\xi_{SS}$  should be of the order of the average spacing between the interstitials or vacancies in the SS. It is interesting to see if neutron or light scattering experiments can test this prediction. Compared to  $E_v^{SF}$ , there are two reductions, one is the superfluid density, another is the increase of the vortex core size  $\xi_{SS} \gg \xi_{SF}$ . These two factors contribute to the very low critical velocity  $v_c^{SS} \sim 30 \mu\text{m/s}$ . Of course, the reduction from the increase of the vortex core is negligible because of the logarithmic dependence.

## VIII. X-RAY SCATTERING FROM THE SS

Let's look at the prediction of our theory on X-ray scattering from the SS. For a lattice with  $j = 1, \dots, n$  basis located at  $\vec{d}_j$ , the geometrical structure factor at the reciprocal lattice vector  $\vec{K}$  is  $S(\vec{K}) = \sum_{j=1}^n f_j(\vec{K}) e^{i\vec{K}\cdot\vec{d}_j}$

where  $f_j$  is the atomic structure factor of the basis at  $\vec{d}_j$ . The X-ray scattering amplitude  $I(\vec{K}) \sim |S(\vec{K})|^2$ . Again, we discuss SS-v and SS-i respectively.

### A. X-ray scattering from the SS-v

In this case, because the superfluid density wave simply sits on the  $n$  lattice, so the X-ray scattering is very similar to that from NS at mean field level. However, as shown in C, quantum and thermal fluctuations will still make the X-ray scattering from the SS-v different from that from the NS.

### B. X-ray scattering from the SS-i

In this case, as shown in section VI, the superfluid density wave is shifted from  $n$  lattice, so the X-ray scattering is different from that from NS even at mean field level. For simplicity, we first take the *sc* lattice to explain the main points, then list the X-ray scattering from all the other lattices classified in section VI.

(a) Simple Cubic lattice. For the SS in the *sc* lattice, as shown in (c2) of the last section, the local superfluid density attains its maximum at the dual lattice points of the *sc* lattice. Then  $\vec{d}_1 = 0, \vec{l}_1 = \frac{a}{2}(\vec{i} + \vec{j} + \vec{k}), \vec{K} = \frac{2\pi}{a}(n_1\vec{i} + n_2\vec{j} + n_3\vec{k})$ , then taking the ratio of the geometric structure factor of SS over that of the NS  $S_{SS}(\vec{K})/S_{NS} = 1 + f(-1)^{n_1+n_2+n_3}$  where  $f \sim \rho_s^{max} \sim a^2$ . It is  $1 + f$  for even  $\vec{K}$  and  $1 - f$  for odd  $\vec{K}$ .

(b) Triangular lattice.  $\vec{d}_1 = 0, \vec{l}_1 = \frac{1}{3}(\vec{a}_1 + \vec{a}_2), \vec{l}_2 = \frac{2}{3}(\vec{a}_1 + \vec{a}_2), \vec{K} = n_1\vec{b}_1 + n_2\vec{b}_2$ , then taking the ratio of the geometric structure factor of SS over that of the NS  $S_{SS}(\vec{K})/S_{NS} = 1 + 2f \cos \frac{2\pi}{3}(n_1 + n_2)$ . This result could be relevant to possible 2d excitonic superfluid in electron-hole bilayer system to be briefly mentioned in section X.

(c) *hcp* lattice. *hcp* lattice is not a Bravais lattice. In NS,  $\vec{d}_1 = 0, \vec{d}_2 = \frac{1}{3}(\vec{a}_1 + \vec{a}_2) + \vec{a}_3/2, \vec{K} = n_1\vec{b}_1 + n_2\vec{b}_2 + n_3\vec{b}_3$ , then  $S_{NS}(\vec{K}) = 1 + e^{i2\pi(\frac{n_1+n_2}{3} + \frac{n_3}{2})}$ . In the SS, there are 2 more additional basis at  $\vec{l}_1 = \frac{2}{3}(\vec{a}_1 + \vec{a}_2) + \vec{a}_3/4, \vec{l}_2 = 3\vec{a}_3/4$ , then  $S_{SS}(\vec{K}) = S_{NS}(\vec{K}) + f e^{i2\pi(\frac{2(n_1+n_2)}{3} + \frac{n_3}{4})} + f e^{i\frac{3\pi}{2}n_3} = S_{NS}(\vec{K}) + f e^{-i\frac{\pi}{2}n_3} S_{NS}^*(\vec{K})$ .

(d) *bcc* lattice. We think *bcc* lattice as a *sc* lattice plus a basis,  $\vec{d}_1 = 0, \vec{d}_2 = \frac{a}{2}(\vec{i} + \vec{j} + \vec{k}), \vec{K} = \frac{2\pi}{a}(n_1\vec{i} + n_2\vec{j} + n_3\vec{k})$ , Then  $S_{NS}(\vec{K}) = 1 + (-1)^{n_1+n_2+n_3}$  which is 2 for even  $\vec{K}$  and 0 for odd  $\vec{K}$ . In the SS, there are 3 more additional basis at  $\vec{l}_1 = \frac{a}{2}(\vec{i} + \vec{j}), \vec{l}_2 = \frac{a}{2}(\vec{i} + \vec{k}), \vec{l}_3 = \frac{a}{2}(\vec{j} + \vec{k})$ , then  $S_{SS}(\vec{K}) = S_{NS}(\vec{K}) + f[(-1)^{n_1+n_2} + (-1)^{n_1+n_3} + (-1)^{n_2+n_3}]$ .

(e) *fcc* lattice. We think *fcc* lattice as a *sc* lattice plus 3 basis located at  $\vec{d}_1 = \frac{a}{2}(\vec{i} + \vec{j}), \vec{d}_2 = \frac{a}{2}(\vec{i} + \vec{k}), \vec{d}_3 = \frac{a}{2}(\vec{j} + \vec{k}), \vec{K} = \frac{2\pi}{a}(n_1\vec{i} + n_2\vec{j} + n_3\vec{k})$ , then  $S_{NS}(\vec{K}) = 1 + [(-1)^{n_1+n_2} + (-1)^{n_1+n_3} + (-1)^{n_2+n_3}]$ . In the SS, there

is one more additional basis located at  $\vec{l}_1 = \frac{a}{2}(\vec{i} + \vec{j} + \vec{k})$ , then  $S_{SS}(\vec{K}) = S_{NS}(\vec{K}) + f(-1)^{n_1+n_2+n_3}$ . It is easy to see that in *bcc* and *fcc* lattices, we need simply exchange  $d$  vectors for the NS and the  $l$  vectors for SDW.

We conclude that the elastic X-ray scattering intensity from the SS-i has an additional modulation over that of the NS. The modulation amplitude is proportional to the maxima of the superfluid density  $\rho_s^{max} \sim a^2$  which is the same as the NCRI observed in the PSU's torsional oscillator experiments.

### C. Effects of Debye-Waller factors on SS-v and SS-i

Due to large zero-point motion in solid  ${}^4\text{He}$ , any X-ray scattering amplitude  $I(\vec{K})$  will be diminished by a Debye-Waller factor. As shown in the last section, because the lattice phonon modes  $\vec{u}$  in  $\psi$  are *locked* to those of  $n$ , so there is a *common* Debye-Waller factor  $\sim e^{-\frac{1}{3}K^2\langle u^2 \rangle}$  coming from the large zero point motions in NS and SS. *If ignoring the coupling between the superfluid  $\theta$  mode and the phonon  $\vec{u}$  mode*, then by taking the ratio  $I_{SS}/I_{NS}$ , we expect this Debye-Waller factor drops out. However, the coupling may still make the Debye-Waller factors in SS-v and SS-i different than that in NS. How the Debye-Waller factor affects the X-ray scattering from the SS-v and SS-i will be discussed in<sup>27</sup>.

Unfortunately, so far, the X-ray scattering data is limited to high temperature  $T > 0.8K > T_{SS}$ <sup>33</sup>. X-ray scattering experiments on lower temperature  $T < T_{SS}$  are being performed to test these predictions<sup>11</sup>.

## IX. THE NCRI OF SF AND SS STATES AT $T = 0$ AND $T > 0$ .

In order to calculate the superfluid density  $\rho_s$  explicitly, we need to look at how the system's free energy responds to a fictitious gauge potential  $\vec{A}$ . We find that when  $\Delta \gg \Delta_c$ ,  $\rho_s(T = 0) = \rho = \int d^d x |\psi(\vec{x}, \tau)|^2 = \int d^d x (|\psi_1(\vec{x}, \tau)|^2 + |\psi_2(\vec{x}, \tau)|^2)$  where the crossing terms between  $\psi_1$  and  $\psi_2$  drop out due to the momenta conservation. Note that although  $\psi_2$  does not contribute to the condensate, it does contribute to the superfluid density. This is consistent with the fact that although 90%  ${}^4\text{He}$  are out of the condensate, they all contribute to the superfluid density.

In the SF state, at low  $T$ , the quantum fluctuations induced by the pressure are important. Let's first look at the quantum phase fluctuations. The phase fluctuation action is given by  $\mathcal{L}_p = \frac{1}{2g} \frac{1}{\beta} \sum_{i\omega_n} \int \frac{d^d k}{(2\pi)^d} (\omega_n^2 + k^2) |\theta(\vec{k}, \omega_n)|^2$  where  $g = \frac{1}{\rho_s}$  controls the strength of quantum phase fluctuations and the superfluid phonon velocity has been set equal to 1 for simplicity. It is easy to see that at  $T = 0$ ,  $\langle \theta^2(\vec{x}, \tau) \rangle_{T=0}$  is infra-red (IR) finite, so the quantum phase fluctuations alone will not

lead to any instability. However, it will lead to superfluid density depletion even before reaching the phase boundary of SF to SS transition in Fig.2 and Fig.3, although the depletion may be quite small. This fact explains why  $T_{SF}(p)$  bends to the left slightly as the pressure  $p$  increases. At finite  $T$ , the thermal fluctuations  $\langle \theta^2(\vec{x}, \tau) \rangle_T - \langle \theta^2(\vec{x}, \tau) \rangle_{T=0} \sim T^{d-1}$  lead to  $\rho_s(T) = \rho_s(T = 0) - cT^2$  at  $d = 3$ . It is well known the superfluid density  $\rho(T) \sim \rho(T = 0) - aT^4$ , while the Bose condensation density  $n_b(T) \sim n_b(T = 0) - bT^2$ . So strictly speaking,  $\psi$  sector can only describe the Bose condensation density. This is expected, because the  $n$  sector in the SF phase also contributes to the superfluid density, but not to the BEC.

Then let's look at the roton fluctuations whose action is given by Eqn.8. Setting  $\Delta_2 = \Delta^2$ , at  $T = 0$ , the quantum roton fluctuations  $\langle \phi_2^2(\vec{x}, \tau) \rangle_{T=0} \sim \log \frac{\Lambda}{\Delta}$  is IR logarithmic divergent as  $\Delta \rightarrow 0$  which signifies the instability to the lattice formation. Due to this IR divergence, the 1st order SF to SS transition may happen well before  $\Delta$  becomes zero, namely, at  $\Delta = \Delta_c > 0$ . This is consistent with the picture described in sec. IV. At finite  $T$ , the thermal roton fluctuations  $\langle \phi_2^2(\vec{x}, \tau) \rangle_T - \langle \phi_2^2(\vec{x}, \tau) \rangle_{T=0} \sim (\log \frac{\Lambda}{\Delta}) e^{-\frac{\Delta}{T}}$  when  $T \ll \Delta \ll \Lambda$ .

In the SS-v and SS-i states, the  $n(x)$  forms a lattice, at the same time, the unstable roton part is replaced by a stable SDW formation commensurate with the underlying  $n$  lattice. Obviously, the  $n(x)$  normal lattice takes away the vast majority of density from the superfluid density even at  $T = 0$ . The preliminary calculations in<sup>27</sup> showed that superfluid density from the  $\psi_1$  sector is isotropic  $\rho_1 \sim Ka^2$ , while the superfluid density from  $\psi_2$  sector turns out to be anisotropic in *hcp* lattice  $\rho_{2,ij} \sim \sum_{m=1}^P |\Delta_m|^2 Q_{mi} Q_{mj} / Q^2$  where  $\Delta_m = \pm a/P$  for SS-v or SS-i. Therefore, the total superfluid density in SS phase is  $\rho_{ij}^{SS} \sim \rho_1 \delta_{ij} + \rho_{2,ij} \sim a^2 (K \delta_{ij} + \frac{1}{P^2} \sum_{m=1}^P Q_{mi} Q_{mj} / Q^2)$ . Taking  $P = 6$ , the anisotropy is quite small. Solid  ${}^4\text{He}$  in a bulk takes a *hcp* lattice with  $c/a \sim 1.63$  which is quite close to the idea value  $c/a = \sqrt{8/3}$ . The three primitive reciprocal lattice vectors are  $G_1 = G_2 = \frac{4\pi}{\sqrt{3}a}$ ,  $G_3 = \frac{2\pi}{c}$ . We can estimate the anisotropy of the NCRI in the *hcp* lattice. If the rotation axis is along the  $c$  axis, the NCRI is  $\rho_{11} \sim Ka^2 + v_r \sum_{m=1}^6 |\Delta_m|^2 Q_{m1} Q_{m1} / Q^2$ . If the rotation axis is along the  $a$  (or  $b$ ) axis, the NCRI is  $\rho_{33} \sim Ka^2 + v_r \sum_{m=1}^6 |\Delta_m|^2 Q_{m3} Q_{m3} / Q^2$ . The anisotropy mainly comes from the  $\psi_2$  sector. Setting  $s = G_1/G_3$ , for the idea value  $s = \frac{4\sqrt{2}}{3} > 1$ , so  $\rho_{11} > \rho_{33}$ . Namely, the NCRI response is larger when one is rotating the sample around the  $c$  axis than that when one is rotating the sample around the  $a$  or  $b$  axis. However, as the pressure is increased,  $s$  decreases, the anisotropy of the NCRI also decreases. In the PSU experiments, the samples are poly-crystal, the relative orientation of the rotation axis to the  $c$  axis is not known, so it's hard to test this prediction with poly-crystals.

## X. DISCUSSIONS ON PSU'S AND OTHER EXPERIMENTS AND APPLICATIONS IN OTHER SYSTEMS

### 1. The effects of He3 impurities

Although the NS to SS transition is in the same universality class as the NL to SF one, it may have quite different off-critical behaviours due to the SDW structure in the SS state. We can estimate the critical regime of the NS to SS transition from the Ginsburg Criterion  $t_G^{-1} \sim \xi_{SS}^3 \Delta C$  where  $\Delta C$  is the specific jump in the mean field theory. Because of the cubic dependence on  $\xi_{SS}$ , large  $\xi_{SS}$  leads to extremely narrow critical regime, the 3D XY critical behavior is essentially irrelevant, instead mean field Gaussian theory should apply. Assuming  ${}^3\text{He}$  impurities diffusion process is slow, we can use this fact to address two experimentally observable effects of the He3 impurities. As said in the introduction, the first one was already observed by the PSU experiments<sup>11</sup>. The second one was just being observed<sup>11</sup>. (1) slightly below  $T_{SS}$ , the vortex pairs are in the dilute vortex limit where the unbinding transition temperature  $T_{SS}$  is determined by the pinning due to impurities instead of by the logarithmic interactions between the vortices which is proportional to the superfluid stiffness. So the He3 impurities effectively pin the vortices and raise the unbinding critical temperature  $T_{SS}$ . Taking the He3 impurity concentration  $x \sim 0.3ppM$ , the average distance  $d_{imp}$  between the He3 impurities is  $d_{imp} \sim 450\text{\AA} \sim 120a$ , the average distance between a vortex pair is  $R_p > \xi_{SS} \gg a$ , we expect  $R_p \sim d_{imp}$ , the vortex pair is indeed effectively pinned by the He3 impurities at such a tiny concentration. On the other hand, He3 impurities will certainly decrease the superfluid density in both the  $\psi_1$  and  $\psi_2$  sector just like He3 impurities decrease superfluid density in the  ${}^4\text{He}$  superfluid. Note that in  ${}^4\text{He}$  superfluid, slightly below  $T_{SF}$ , the vortex pairs are in the dense vortex limit where the unbinding transition temperature  $T_{SF}$  is determined by the logarithmic interactions between the vortices which is proportional to the superfluid stiffness. So in  ${}^4\text{He}$  SF, He3 impurities hurt superfluid density which, in turn, lead to the reduction in  $T_{SF}$ . In short, the He3 impurities play a dual role in the SS phase, on the one hand, they raise the unbinding critical temperature  $T_{SS}$  of the vortices, on the other hand, they decrease the superfluid density in both  $\psi_1$  and  $\psi_2$  sector. Indeed, in the PSU's experiments, in an isotropically stressed sample, as the concentration of He3 impurities decreases, the  $T_{SS}$  drops considerably, but the NCRI rises. In contrast, in both 3d superfluid  ${}^4\text{He}$  and 2d superfluid  ${}^4\text{He}$  films, He3 impurities hurt both the superfluid stiffness and  $T_c$ . So the role played by He3 impurities in the PSU experiments is similar to the disorder played in fractional quantum Hall effects: the disorder is needed to even have a fractional quantized Hall plateau, but the quantum Hall liquid ground state is completely due to the strong Coulomb interaction among electrons and exists even in the absence of disorder. How-

ever, too much disorder will also destroy the fractionally quantized Hall plateau just like too much He3 impurities will also destroy the superfluid density. (2) In principle, in clean system, the specific heat measurement should show the  $\lambda$  peak as the NL to SF transition does. Because the 3d XY specific heat exponent  $\alpha = -0.012 < 0$ , from the Harris criterion, we conclude that weak disorder will not change the universality class of the 3d XY model describing the SS to the NS transition, so will not destroy the  $\lambda$  peak. However, due to very narrow critical regime, it will be very difficult to observe the  $\lambda$  peak. So the 3D XY critical behavior of the NS-SS transition is essentially irrelevant in the PSU experiments, instead mean field Gaussian theory should apply where there should be a specific heat jump at  $T = T_{SS}$ . The mean field jump maybe smeared by the presence of He3 impurities. Indeed, recent very refined specific heat measurements indeed found a broadened specific heat peak around  $\sim 100mK$  when  $x \sim 0.3 - 3ppM$ <sup>11</sup>. We conclude that the broadened specific heat peak around  $\sim 100mK$  in the presence of He3 impurities is closely related to the opposite trend of the dependence of  $T_{SS}$  and the superfluid density on the concentration of He3 impurities.

### 2. Non-equilibrium behavior in the torsional oscillator experiments

In principle, the superfluid density should scale as  $\rho_s \sim (T_c - T)^\nu$  in the critical regime where  $\nu \sim 0.67$  for the 3D XY model. Again, due to the very narrow critical regime, this scaling will not be seen. The experiment<sup>8</sup> found that the NCRI slides towards to the normal solid side with a very long tail. As argued in<sup>15</sup>, this behavior may be attributed to the non-equilibrium effects of the torsional oscillator experiments.

### 3. Other torsional oscillator, mass flow and acoustic wave experiments

Recently, a Cornell group lead by Reppy found that the NCRI signal detected by the PSU group can be eliminated through a crystal annealing process<sup>16</sup>. There are two possible explanations for this observation (1) This corresponds to  $v < v_c$  where the Fig.3 holds. There could be vacancies or interstitials in the thermodynamic stable ground state whose condensation leads to the SS in the Fig.3. The annealing process simply push the He3 impurities to the boundary, so reduces the supersolid transition temperature  $T_{SS}$  as discussed in this section. (2) This corresponds to  $v_i > v_{ic}$  where the Fig.2 holds. A state with vacancies or interstitials is just a metastable state, then the supersolid state is just a metastable state. Annealing not only gets rid of the He3 impurities, but also vacancies or interstitials, so reduce or eliminate the metastable SS state. Even so, a SS metastable state maybe interesting and deserves the investigations done in this paper. Note that the Cornell's experiment itself may be controversial. The PSU group did the same annealing process which, in fact, last much longer than Cornell's group did, so should result even better crystal with even better quality, but the supersolid signal ( NCRI effect ) stays more or less the same<sup>11</sup>. One of the

main points of the manuscript is that the X-ray scattering experiment on SS-v or SS-i, if can be performed at low enough temperature, can be very helpful to resolve the debate.

Beamish's group<sup>17</sup> found that there is no detectable mass flow driven by pressure difference in solid Helium in Vycor at temperature as low as 48 mK and pressure 60 bar. It is possible that the response of the SDW in the SS to the pressure difference may be quite different than a uniform SF. It is important to work out this response. In another word, it is important to resolve the puzzle that why the SDW behaves like a superfluid in the torsional oscillator experiment, but does not response sensitively to a pressure difference.

By acoustic attenuation and heat wave experiments<sup>38</sup>, Goodkind discovered that the solid  ${}^4\text{He}$  displays a phase transition below 200 mK only if it is strained or in the presence of  $\text{He3}$  impurities also in the concentration range of  $\sim ppM$ . This observation is consistent with the PSU's torsional oscillator experiments. The mechanism proposed above may also lead to a natural explanation of Goodkind's observation.

#### 4. Comparisons with Supersolids on lattices

Supersolids on lattice models were studied in<sup>39</sup>. The GL theory, especially the coupling between  $n$  sector and  $\psi$  sector in<sup>39</sup> are different than those in Eqn.1, Eqn.2, Eqn.3 in bulk  ${}^4\text{He}$  system constructed in this paper. In<sup>39</sup>, due to the lack of  $\psi$  components in non-zero reciprocal lattice vectors  $\vec{G}$ , the first non-trivial coupling is in quartic term  $\sum_{\vec{G}} v_{\vec{G}} |n_{\vec{G}}|^2 |\psi|^2$  instead of the cubic term in Eqn.3. This crucial difference make the two GL theories completely differently.

In<sup>40</sup>, we studied all the possible phases and phase transitions in an extended boson Hubbard model in bipartite lattices such as a honeycomb and square lattice near half filling. We show that there are two consecutive transitions at zero temperature *driven by the chemical potential*: in the Ising limit, a Commensurate-Charge Density Wave (CDW) at half filling to a narrow window of CDW supersolid, then to an Incommensurate-CDW; in the easy-plane limit, a Commensurate-Valence Bond Solid (VBS) at half filling to a narrow window of VBS supersolid, then to an Incommensurate-VBS. The first transition is second order in the same universality class as the Mott to insulator transition, therefore has the exact critical exponents  $z = 2, \nu = 1/2, \eta = 0$  with logarithmic corrections, while the second one is first order. Liu and Fisher<sup>39</sup> also studied the C-CDW to the CDW-SS transition and concluded that  $z = 1$  in contrast to  $z = 2$  achieved in<sup>40</sup>. We found that the phase diagram in the Ising limit is similar to the reentrant "superfluid" in a narrow region of coverages in the second layer of  ${}^4\text{He}$  adsorbed on graphite detected by Crowell and Reppy's torsional oscillator experiment in 1993<sup>42</sup>. It is still not clear if the extended boson Hubbard model can describe the experimental situation well. But the results suggest that  ${}^4\text{He}$  lattice supersolid may have been already observed in 1993 which was 11 years earlier than the PSU's

experiments on bulk  ${}^4\text{He}$ . Indeed, the data in the torsional oscillator experiment in<sup>42</sup> do not show the characteristic form for a 2d  ${}^4\text{He}$  superfluid film, instead it resembles that in<sup>7</sup> characteristic of a supersolid in terms of the gradual onset temperature of the NCRI, the unusual temperature dependence of  $T_{SS}$  on the coverage. Of course, both experiments may due to phase separations instead of the SS phase. very recently, the author studied various kinds of supersolids in frustrated lattices such as triangular and kagome lattices<sup>41</sup>.

It is known that a lattice system is different than a continuous system in many ways. So the reentrant lattice SS discussed in<sup>39,40,41</sup> is different from the bulk  ${}^4\text{He}$  SS state discussed in this paper, although both kinds of supersolids share many interesting common properties. In both cases, the SF to SS transition is driven by the closing of the gap of the roton minimum. On the lattice, the manifold of the roton minimum consists of discrete points due to the lattice symmetry, so the transition could be 1st or second order. However, in  ${}^4\text{He}$ , as shown in sections III and IV, the manifold of the roton minimum is a continuous surface, so the transition must be first order. In the former, there is a periodic substrate or spacer potential which breaks translational symmetries at the very beginning. The filling factor is controlled by a external chemical potential. There are particle-hole symmetry for excitations at integer filling factors which ensure the number of particles is equal to that of vacancies and at half filling factors which ensure adding interstitials is equivalent to adding vacancies<sup>40,41</sup>. While in the latter, the lattice results from a spontaneous translational symmetry breaking driven by the pressure as shown in the Fig.3, the filling factor has to be self-determined by ground state energy minimization. There is usually no particle-hole symmetry for excitations except at some specific pressures. Due to this absence of symmetry, the number of vacancies is usually not equal to that of interstitials. So the theory developed in this paper on bulk  ${}^4\text{He}$  is different from the lattice theory developed in<sup>39,40</sup>. As shown in the appendix and in<sup>40,41</sup>, one common fact of both supersolids is that both are due to vacancies or interstitials. It is not known if local tunneling processes can also lead to supersolids in bulk  ${}^4\text{He}$  at commensurate filling factors. However, it was shown in<sup>41,48</sup>, lattice supersolids exist even at commensurate 1/2 filling factors in frustrated lattices such as triangular lattice. Combined with the results in<sup>40</sup>, we conclude that  ${}^4\text{He}$  supersolid can exist both in bulk and on substrate, while although  $H_2$  supersolid may not exist in the bulk, but it may exist on wisely chosen substrates. Lattice supersolid could also be realized in optical lattices in ultra-cold atomic experiments<sup>6,45</sup>. However, in both continuum and on lattices, SS states could be unstable against phase separations. For example, the vacancies or interstitials in the in-commensurate solid can simply move to the boundary of the sample instead of boson condensation, namely, it will turn into a commensurate solid. This case is included in the  $v_i > v_{ic}$  case in the paper any-

way. Due to its negative compressibility, the instability of lattice SS against phase separation was demonstrated in some lattice models in<sup>46,47</sup>.

### 5. Absence of supersolid in solid hydrogen

The solid (para)-hydrogen  $H_2$  also takes the *hcp* lattice. As explained in the introduction, so far, no NCRI was discovered in  $H_2$  solid. Although  $H_2$  are even lighter than  $^4He$ , it has deeper attractive potential, so smaller de Boer quantum number. Bulk  $H_2$  solidifies at  $T < T_c \sim 14K$  even at zero pressure, this fact preempts the possible observation of the speculated SF state. At  $T = 0$ , due to the absence of the adjacent SF state, the quantum fluctuations are not strong enough to produce vacancies or interstitials in the  $H_2$  solid, so the solid is a commensurate solid. Therefore, no SS is possible. As shown in section VI,  $T_{SS} < T_{SF}$ , if  $T_{SF} = 0$ , then  $T_{SS} = 0$ . Namely, in a continuous system, a SS state can not exist without the existence of an adjacent SF state in the first place. One potential avenue to prevent  $p - H_2$  from being solidified to low enough temperature such that the superfluid behavior can be observed is by depositing  $H_2$  on external substrates which can disrupt the deep  $H_2$  potential. It was suggested in<sup>40</sup> that a judicious choice of substrate may be able to lead to an occurrence of hydrogen lattice supersolid.

### 6. Possible excitonic supersolids in fermionic systems

Although 2d bilayer quantum Hall system ( BLQH ) is a fermionic system, it was argued there exists excitonic superfluid (ESF) state in the pseudo-spin channel<sup>49</sup>. In real space, one exciton is an electron in one layer paired with a hole in another layer ( with respect to the underlying  $\nu = 1$  integer quantum Hall state ), its size is of the same order of the interlayer distance, so could be viewed as a boson in the pseudo-spin channel. In<sup>50,51,52</sup>, starting from the ESF state, as the distance increases, we studied the instability due to the collapsing of the magneto-roton minimum at  $q_0$  which leads to the formation of the pseudo-spin density wave (PSDW). We showed that a square lattice is the favorite lattice for the PSDW. The interlayer distance in BLQH play a similar role as the pressure in  $^4He$ . Unlike in  $^4He$  where the lattice constant is determined by the pressure, the lattice constant  $a$  of the resulting PSDW is completely fixed by the filling factor which is independent of the distance, due to the slight mismatch between the lattice constant  $a$  and the instability point  $1/q_0$ , the resulting PSDW is likely to be an *in-commensurate* solid where the number of sites  $N_s$  may not be the same as the number of excitons  $N$  even at  $T = 0$ . As the distance increases further  $d_{c1} < d < d_{c2}$ , the PSDW lattice constant is still *locked* at the same value  $a$ . Assuming zero-point quantum fluctuations favor vacancies over interstitials, we take  $N < N_s$ , so there are vacancies  $n_0$  even at  $T = 0$  in both top and bottom layers. As argued in<sup>50</sup>, the correlated hopping of vacancies in the active and passive layers in the PSDW state leads to very large and temperature dependent drag consistent with the experimental data. However an excitonic supersolid (ESS) is very unlikely in BLQH. In sym-

metric electron-hole bilayer systems<sup>53</sup>, it was shown in<sup>54</sup> that it is quite possible that there may a narrow window of ESS where both order parameters are non-vanishing  $\langle \psi \rangle \neq 0, \langle n_{\vec{c}} \rangle \neq 0$  intervening between the ESF and an excitonic normal solid ( ENS ).

In fermionic systems, it is easy to see the coexistence of CDW and Superconductivity ( SC), so " fermionic supersolid " phases are common. For instance, a quasi-two-dimensional system NbSe2 has a transition to an incommensurate CDW phase at some high temperature  $T_{CDW}$  and then a transition to a phase with coexisting CDW and SC order at a lower temperature  $T_{SC}$ . The CDW is a pairing in particle-hole channel at  $2k_F$ , its order parameter is  $\psi_{CDW} = \langle c_{\uparrow}^{\dagger}(\vec{k})c_{\sigma}(\vec{k} + \vec{Q}) \rangle$  where  $\vec{Q}$  is the ordering wave vector of the CDW. The SC is a pairing in particle-particle channel also across the Fermi surface. Its order parameter is  $\psi_{SC} = \langle c_{\uparrow}^{\dagger}(\vec{k})c_{\downarrow}^{\dagger}(-\vec{k}) \rangle$ . Both order parameters are composite order parameters. Different parts of Fermi surface can do the two jobs separately ( see, for example,<sup>55</sup> ). In contrast to the bosonic SS where there is a density operator  $n$  and a complex order parameter  $\psi$ , both order parameters  $\psi_{CDW}$  and  $\psi_{SC}$  are complex order parameters. We can see that the formation of a supersolid in a bosonic system has completely different mechanism as shown in this paper, so the QGL theories in the fermionic and bosonic systems could be different to a large extent. it would be interesting to construct a QGL theory to describe the interplay between the two complex order parameters, the properties of the "fermionic supersolid" (FSS) and the transition from the FSS to the CDW. However, the fermionic excitations near the nodes maybe important<sup>55</sup>.

## XI. CONCLUSIONS

The PSU's experiments renewed the interests in the  $^4He$  system which already had fantastic properties. In this paper, we constructed a two component QGL theory to map out the  $^4He$  phase diagram, analyze the conditions for the existence of the supersolid and study all the phases and phase transitions in a unified view. We developed the theory basing on the two facts (1) there is a roton minimum in the superfluid state (2) the instability to solid formation is driven by the gap diminishing at the roton minimum. The only new parameter introduced in the GL theory this paper is the coupling between the  $n$  sector ( or normal solid part ) and the  $\psi$  sector ( or the superfluid part ) in Eqn.3. Depending on the sign and strength of the repulsive coupling  $v_1$  between the solid and superfluid, we found two possible scenarios: (1) If the coupling is larger than a critical value  $v > v_c$  ( Fig.1 ), then the resulting solid at  $T = 0, p > p_c$  is a commensurate normal solid. The SS state does not exist as a ground state. However, it may still exist as a metastable state. The QGL action to describe this SF to NS transition in Fig.2 was developed in Sec.IV. (2) If the coupling is smaller than a critical value  $v < v_c$ , the resulting solid

at  $T = 0, p > p_c$  is an incommensurate solid with zero point quantum fluctuations generated vacancies if it is negative and interstitials if it is positive ( Fig.1). The condensation of the vacancies or interstitials lead to the formation of the SS-v and SS-i respectively. The SS state has lower energy than the NS state at  $T = 0$ . Our results on supersolid should be independent of many microscopic details and universal. We investigated the SS state from both the SF and the NS side and found completely consistent description of the properties of the SS state. By increasing the pressure from the superfluid side, the superfluid (SF) to supersolid ( SS ) transition in Fig.3 is a simultaneous combination of the SDW transition in the  $\psi$  sector driven by the roton condensation at  $k_0 = k_r$  and the NS transition in the  $n$  sector driven by the divergence in the structure function  $k_0 = k_n = k_r$ . The superfluid becomes a SS at lower temperature and a NS at higher temperature ( Fig.3 ). We also approached the SS state from the NS side and found that the NS to SS transition is described by a 3d XY model with much narrower critical regime (Fig.3).

Finally, it may be instructive to make some analogy of Fig.2 and Fig.3 at  $T < T_{SF}$  to Type I and type II superconductors with the pressure  $p$  playing the role of the magnetic field  $H$ : Fig.2 is similar to Type I superconductor with SF identified as the Messiner state, the NS as the normal state, the critical pressure  $p_c$  identified as the critical magnetic field  $H_c$ . Fig.3 is similar to Type II superconductor with SF identified as the Messiner state, the SS as the mixed vortex lattice state which also breaks both translational order and the global  $U(1)$  symmetry, the NS as the normal state, the lower and upper critical pressures  $p_{c1}$  and  $p_{c2}$  identified as the lower and upper critical magnetic fields  $H_{c1}$  and  $H_{c2}$ . In superconductors, it is the  $\kappa = \lambda/\xi$  to determine type I and Type II and if the vortex lattice is a stable intermediate state or not as the magnetic field is increased. In Helium 4, it is the sign and strength of the coupling constant  $v$  in Eqn.3 to determine the Fig.2 and Fig.3 and if the SS is a stable intermediate state or not as the pressure is increased. This analogy works even better with SS-i supersolid with  $v$  playing a similar role as  $1/\kappa$ .

Just like the SF is a uniform two-component phase consisting of superfluid and normal component at any finite temperature, the SS state is a uniform two-component phase consisting of a superfluid density wave (SDW) and a normal solid component even at zero temperature. The SDW in the SS-v coincides with the underlying normal solid. While the SDW in the SS-i state is just a dual lattice to the underlying normal solid. This important fact leads to the key prediction in this paper: the X-ray scattering intensity from the SS-v is similiar to that of NS at mean field level, while the X-ray scattering intensity from the SS-i ought to have an additional modulation over that of the NS. The modulation amplitude is proportional to the Non-Classical Rotational-Inertial (NCRI) observed in the torsional oscillator experiments. This prediction is amenable to ongoing X-ray scattering experiments on

$^4\text{He}$  at very low temperature. The important effects of Debye-Waller factors on SS-i and SS-v are discussed and will be calculated in future publications<sup>27</sup>. The NCRI is only weakly anisotropic in the SS phase for *hcp* lattice. The fact that the critical regime of the NS to SS transition is much narrower than the NL to SF transition leads to the two experimentally observable effects of He3 impurities. (1) The He3 impurities decrease the superfluid density, but increase the critical temperature transition  $T_{SS}$  from the SS to the NS transition. (2) The He3 impurities may smear specific heat jump at  $T = T_{SS}$  into a broad peak. Indeed, an excessive specific heat anomaly around  $\sim 100 \text{ mK}$  has been detected in very recent refined experiments in the samples with  $x \sim 0.3 - 3 \text{ ppM}$  at PSU<sup>11</sup>. By studying all the phases in a unified framework, we conclude there is no SS in hydrogen. We also made comments on several other experiments.

If the supersolid state is responsible for the NCRI observed in PSU's experiments remains controversial. The GL theory developed in this paper put the competing orders of superfluid and solid in the unified framework. It can be used to address many questions raised in PSU's experiments and other experiments and to make predictions to be tested by future experiments. It can also be applied to study possible supersolid state in other continuous bosonic and electronic systems such as BLQH and electron-hole bilayer system. We suggest that even supersolid may not be realized in  $^4\text{He}$  system, it has its own intrinsic, deep and profound scientific interests and impacts and may be realized in other continuous bosonic and fermionic systems.

#### Acknowledgement

I am deeply indebted to Tom Lubensky for patiently explaining to me the physics of liquid crystal and many insightful and critical comments on the manuscript. I thank P. W. Anderson, M. Chan, T. Clark, Milton Cole, B. Halperin, Jason Ho, J. K. Jain, S. Kivelson, T. Leggett, Mike Ma, G. D. Mahan, S. Sachdev and F. C. Zhang for helpful discussions, A. T. Dorsey for pointing out Ref.<sup>22</sup> to me, R. X. Li for technical assistance. I also thank all the participants for many heated and fruitful discussions during the two weeks mini-workshop on supersolid held at KITP at UC Santa Barbara organized by D. M. Ceperley and M. Chan. The research at KITP was supported by the NSF grant No. PHY99-07949. I also thank the hospitality of Y. Chen, Z. Wang and F. C. Zhang during my visit at Hong Kong University, Yu Lu and Xiang Tao during my visit at Institute for Theoretical Physics in Beijing, China.

#### APPENDIX A: DISCUSSIONS ON A TOY SUPERSOLID GROUND STATE WAVEFUNCTION

The Ginzburg-Landau theory constructed in the main text is based on order parameters and symmetries. It should hold irrespective many microscopic details such

as what is the mechanism responsible for the formation of the supersolid. Despite there are many microscopic calculations for  ${}^4\text{He}$ , constructing a microscopic theory for supersolid is very difficult. In this appendix, I will discuss a well known toy SS wavefunction and clarify a few concepts related to *global* phase-number uncertainty relation and the role of vacancies or interstitials in the formation of SS. We also clarify the physical meaning of the order parameters  $n$  in Eqn.1 and  $\psi$  in Eqn.2. However, because the toy wavefunction may miss some important physics in bulk  ${}^4\text{He}$  systems. For example, due to the very peculiar potential well in the solid  ${}^4\text{He}$  which has a local shallow maximum at the lattice site, the tight binding model is very crude, Eqn.A1 is built on a rigid lattice, it does not include phonon excitations, so the discussion is very intuitive and crude.

Inside the SF state, because of the strong hard core and long-range correlations between the bare  ${}^4\text{He}$  atoms, the order parameter  $\psi$  in Eqn.2 is related to, but should not be taken as the bare  ${}^4\text{He}$  atom annihilation operator, namely,  $n(\vec{x}) \neq \psi^\dagger(\vec{x})\psi(\vec{x})$ . Inside the NS phase, its physical meaning need some explanations. In this section, we discuss the physical meanings of  $\psi$  and  $n$  in Eqns.1,2,3 inside the SS state from a toy wavefunction of the SS state.

The toy wavefunction of a supersolid takes the BCS like form

$$|SS\rangle = \prod_{i=1}^N (u + vb_i^\dagger) |0\rangle \quad (\text{A1})$$

where  $u \neq 0$  and  $|u|^2 + |v|^2 = 1$ . If setting  $u = 0$ , the state reduces to a commensurate solid without any vacancies  $|CS\rangle = \prod_{i=1}^N b_i^\dagger |0\rangle$ . The commensurate solid (CS) is an exact eigenstate of the boson number operator  $N_b = \sum_{i=1}^N n_i$  with the eigenvalue  $N_b = N$ , so has no chance to become phase ordered. Adding a superfluid component to the CS leads to the SS in Eqn.A1. If setting  $v = 0$ , then the state reduces to the vacuum state  $|0\rangle$ .

If setting  $u = \cos \frac{\theta}{2}, v = \sin \frac{\theta}{2} e^{i\phi}$ , then Eqn.A1 becomes:

$$|SS, \phi\rangle = \prod_{i=1}^N \left( \cos \frac{\theta}{2} + \sin \frac{\theta}{2} e^{i\phi} b_i^\dagger \right) |0\rangle \quad (\text{A2})$$

where  $\theta \neq \pi$ .

By construction, the state has the translational order with the average boson density  $\langle n_i \rangle = |v|^2 = \sin^2 \theta/2$ , so the average vacancy density is  $|u|^2 = \cos^2 \theta/2$ . It is easy to see that  $|SS\rangle$  also has the ODLRO with  $\langle b_i \rangle = u^*v = \frac{1}{2} \sin \theta e^{i\phi}$ , so  $|SS\rangle$  is indeed a supersolid state.

The angle  $\theta$  controls the magnitude, while the phase  $\phi$  controls the phase of the condensation. Defining  $b_{k=0} = \frac{1}{\sqrt{N}} \sum_{i=1}^N b_i$  which satisfy the boson commutation relation  $[b_0, b_0^\dagger] = 1$ , the boson operator at zero momentum is  $n_0 = b_{k=0}^\dagger b_{k=0}$ , the total number of bosons at the zero momentum state is  $N_0 = \langle SS | n_0 | SS \rangle = \frac{N}{4} \sin^2 \theta = N_b \cos^2 \theta/2 < N_b = N \sin^2 \theta/2 < N$ . At integer filling  $n = 1$ , the superfluid state  $|SF\rangle = \frac{1}{\sqrt{N!}} (b_{k=0}^\dagger)^N |0\rangle$ , then  $N_0 = \langle SF | n_0 | SF \rangle = N_b = N$ . Obviously, this SF state is not included in the family in the Eqn.A1.

A supersolid state  $|SS, N_b\rangle$  with  $N_b$  bosons is given by:

$$|SS, N_b\rangle = \int_0^{2\pi} \frac{d\phi}{2\pi} e^{-iN_b\phi} |SS, \phi\rangle \quad (\text{A3})$$

where the total boson number  $N_b$  and the global phase  $\phi$  are two Hermitian conjugate variables satisfying the commutation relation:  $[N_b, \phi] = i\hbar$ . It leads to the uncertainty relation  $\Delta N_b \Delta \phi \geq 1$ .

It is easy to see  $\langle N_b \rangle = \frac{N|v|^2}{2} = N \sin^2 \theta/2, \Delta N_b = \sqrt{\langle N_b^2 \rangle - \langle N_b \rangle^2} = \sqrt{N} |uv| = \sqrt{N} \frac{1}{2} |\sin \theta|, \Delta N_b / \langle N_b \rangle = \frac{1}{\sqrt{N}} |u/v| = \frac{1}{\sqrt{N}} |\cot \theta/2|$ . If  $\theta \neq \pi$ , the absolute boson number fluctuation  $\Delta N_b \sim \sqrt{N}$  is quite large, so  $\Delta \theta$  could be quite small, so one can get a phase ordered state. On the other hand, the relative boson number fluctuation  $\Delta N_b / \langle N_b \rangle \sim \frac{1}{\sqrt{N}}$  is quite small, so one can still measure the average boson number accurately. The first quantization form of the Eqn.A3 can be derived by the same method used in<sup>19</sup>.

Because in the SS state, there is a global phase ordering in  $\phi$ , so its conjugate variable is the total number of particles  $N_b$  as shown in Eqn.A3. The local tunneling or exchanging processes stressed in<sup>4</sup> may not cause the total number fluctuations, therefore may not cause the global phase ordering leading to the supersolid phase. The discussions in this appendix is at most instructive. It is known that state Eqn.A1 may not describe the ground state of the solid  ${}^4\text{He}$  Hamiltonian well, but what it implies is that if the vacancies in an incommensurate solid could lead to the formation of a supersolid. In this indeed happens, in the GL theory constructed for SS-v in the main text, the bosons are represented by  $n(x)$ , while the vacancies are represented by  $\psi$ . A toy wavefunction for SS-i is not written down so far, because the interstitials are moving between lattice sites. In the SS-i, the bosons are represented by  $n(x)$ , while the interstitials are represented by  $\psi$ .

<sup>1</sup> C. N. Yang, Rev. Mod. Phys. **34**, 694 (1962).

<sup>2</sup> A. Andreev and I. Lifshitz, Sov. Phys. JETP **29**, 1107 (1969).

<sup>3</sup> G. V. Chester, Phys. Rev. A **2**, 256 (1970).

<sup>4</sup> A. J. Leggett, Phys. Rev. Lett. **25**, 1543 (1970).

<sup>5</sup> W. M. Saslow, Phys. Rev. Lett. **36**, 1151-1154 (1976).

- <sup>6</sup> For review of NCRI in atomic gases, see Franco Dalfovo, Stefano Giorgini, Lev P. Pitaevskii and Sandro Stringari, *Rev. Mod. Phys.* 71, 463?512 (1999); Anthony J. Leggett, *Rev. Mod. Phys.* 73, 307?356 (2001).
- <sup>7</sup> E. Kim and M. H. W. Chan, *Nature* 427, 225 - 227 (15 Jan 2004).
- <sup>8</sup> E. Kim and M. H. W. Chan, *Science* 24 September 2004; 305: 1941-1944.
- <sup>9</sup> A. Clark and M. H. W. Chan, *J. Low Temp. Phys.* **138**, 853 (2005).
- <sup>10</sup> E. Kim, M. H. W. Chan, *Phys. Rev. Lett.* **97**, 115302 (2006).
- <sup>11</sup> M. H. W. Chan, private communication and to be submitted.
- <sup>12</sup> D. M. Ceperley, B. Bernu, *Phys. Rev. Lett.* **93**, 155303 (2004); N. Prokof'ev, B. Svistunov, *Phys. Rev. Lett.* **94**, 155302 (2005); D. E. Galli, M. Rossi, L. Reatto, *Phys. Rev. B* 71, 140506(R) (2005); Evgeni Burovski, Evgeni Kozik, Anatoly Kuklov, Nikolay Prokof'ev, Boris Svistunov, *Phys. Rev. Lett.*, vol. 94, p. 165301 (2005).
- <sup>13</sup> W. M. Saslow, *Phys. Rev. B* **71**, 092502 (2005); N. Kumar, cond-mat/0507553; G. Baskaran, cond-mat/0505160; Xi Dai, Michael Ma, Fu-Chun Zhang, cond-mat/0501373 ; Hui Zhai, Yong-Shi Wu, *J. Stat. Mech.* P07003 (2005). D.T. Son, cond-mat/0501658.
- <sup>14</sup> A. T. Dorsey, P. M. Goldbart, J. Toner, *Phys. Rev. Lett.* **96**, 055301 (2006).
- <sup>15</sup> P. W. Anderson, W. F. Brinkman, David A. Huse, *Science* 18 Nov. 2005; 310: 1164-1166.
- <sup>16</sup> Ann Sophie C. Rittner, John D. Reppy, Elimination of the Supersolid State Through Crystal Annealing, cond-mat/0604528.
- <sup>17</sup> James Day, T. Herman and John Beamish, *Phys. Rev. Lett.*, vol 95, 035301 (2005).
- <sup>18</sup> I thank Tom Lubensky for discussions leading to the fact that there should be this  $n$  sector in addition to the  $\psi$  sector.
- <sup>19</sup> Gun Sang Jeon and Jinwu Ye, *Phys. Rev. B* 71, 035348 (2005) .
- <sup>20</sup> Jinwu Ye, Density wave states in superfluid, cond-mat/0512480.
- <sup>21</sup> T. Schneider and C. P. Enz, *Phys. Rev. Lett.* 27, 1186 (1971); Yves Pomeau and Sergio Rica, *Phys. Rev. Lett.* 72, 2426 (1994).
- <sup>22</sup> P. Nozieres, *J. Low. Temp. Phys.* 137, 45 (2004).
- <sup>23</sup> Jinwu Ye, *Phys. Rev. Lett.* 97, 125302 (2006).
- <sup>24</sup> Guenter Ahlers, *Phys. Rev. A* 3, 696C716 (1971); Dennis S. Greywall and Guenter Ahlers, *Phys. Rev. A* 7, 2145C2162 (1973).
- <sup>25</sup> It can be easily shown that including both the spin waves and vortex excitations in  $\psi_1$  will not change the following results.
- <sup>26</sup> For discussions on Classical Lifshitz Point (CLP) and their applications in nematic to smectic-A and -C transitions in liquid crystal, see the wonderful book by P. M. Chaikin and T. C. Lubensky, *Principles of Condensed Matter Physics*, Cambridge university press, 1995.
- <sup>27</sup> Jinwu Ye, unpublished.
- <sup>28</sup> I thank Tom Lubensky for discussions leading to the fact that the  $\theta_2$  phase factor is important and may lead to superfluid Goldstone mode.
- <sup>29</sup> R. Shankar, *Rev. Mod. Phys.* 66, 129?192 (1994).
- <sup>30</sup> S. A. Brazovskii, *JETP* 41, 85 (1975).
- <sup>31</sup> Feymann originally conceived the roton as drifting vortex loop. But this point of view is very controversial. If taking this view, then the roton condensation can be considered as vortex loop condensation.
- <sup>32</sup> Neglecting the self interaction  $u$  and taking  $v_i^{NS}$  as a small parameter, A rough estimate on the eigen-energy at the origin  $\vec{K} = 0$  is that  $\epsilon(\vec{K} = 0) = t + v_i^{NS}n_0 - P(v_i^{NS}n_{\vec{c}})^2/KQ^2 + \dots$ . For small  $v_i^{NS}$  and  $n_{\vec{c}}$ , we need only take the first two terms in estimating  $T_{SS}$ . In the strong coupling limit  $v_i^{NS} \rightarrow \infty$ , we expect the results on  $v_i^{NS} > v_{ic}$  in the main text stay the same, although the critical value  $v_{ic}$  may depend on microscopic details. The above calculations do not hold in vacancies case where a tight binding limit is necessary.
- <sup>33</sup> B. A. Fraass, P. R. Granfors, and R. O. Simmons, *Phys. Rev. B* 39, 124C131 (1989). C. A. Burns and E. D. Isaacs, *Phys. Rev. B* 55, 5767C5771 (1997).
- <sup>34</sup> I thank Tom Lubensky for this observation.
- <sup>35</sup> J. E. Hoffman *et al.* *Science* 295, 466 (2002).
- <sup>36</sup> S. R. White and D. J. Scalapino, *Phys. Rev. Lett.* 80, 1272 (1998).
- <sup>37</sup> The core energy is always much smaller than the superflow energy even for large size of vortex core.
- <sup>38</sup> John M. Goodkind, *Phys. Rev. Lett.* 89, 095301 (2002).
- <sup>39</sup> K. S. Liu and M. E. Fisher, *Jour of Low Temp. Phys.* 10, 655, (1973).
- <sup>40</sup> Jinwu Ye, Quantum phase transitions from solids to supersolids in bipartite lattices. cond-mat/0503113.
- <sup>41</sup> Jinwu Ye, Supersolids and solids to supersolids transitions in frustrated lattices. cond-mat/0612009.
- <sup>42</sup> P. A. Crowell and J. D. Reppy, *Phys. Rev. Lett.* 70, 3291C3294 (1993); *Phys. Rev. B* 53, 2701C2718 (1996).
- <sup>43</sup> P.W. Anderson; *Science* 235, 1196(1987).
- <sup>44</sup> H. Wiechert and K. Kortmann, *Phys. Rev. B* 70, 125410 (2004).
- <sup>45</sup> M. Greiner, O. Mandel, T. Esslinger, T. W. Hansch, T. Bloch, *Nature* 415, 39-44 (2002).
- <sup>46</sup> G. C. Batrounil *et al.*, *Phys. Rev. Lett.* 74, 2527 (1995); *ibid.*, 84, 1599 (2000).
- <sup>47</sup> Pinaki Sengupta, *et al.*, *Phys. Rev. Lett.* 94, 207202 (2005).
- <sup>48</sup> Ganpathy Murthy, Daniel Arovas, Assa Auerbach, *Phys. Rev. B* 55, 3104 (1997).
- <sup>49</sup> For a review, see S. M. Girvin and A. H. Macdonald, in *Perspectives in Quantum Hall effects*, edited by S. Das Sarma and A. Pinczuk (Wiley, New York, 1997).
- <sup>50</sup> Jinwu Ye, Quantum Phase transitions in bilayer quantum Hall systems at total filling factor  $\nu_T = 1$ , cond-mat/0606639.
- <sup>51</sup> Jinwu Ye, Fractional charges and quantum phase transitions in imbalanced bilayer quantum Hall systems. *Phys. Rev. Lett* 97, 236803 (2006).
- <sup>52</sup> Jinwu Ye, Mutual Composite Fermion and Composite Boson approaches to balanced and im-balanced bilayer quantum Hall systems: an electronic analogy of Helium 4 system, cond-mat/0310512.
- <sup>53</sup> L. V. Butov, C. W. Lai, A. L. Ivanov, A. C. Gossard, D. S. Chemla, L. V. Butov, A. C. Gossard, D. S. Chemla, *Nature* 418, 751 - 754 (15 Aug 2002). D. Snoke, S. Denev, Y. Liu, L. Pfeiffer, K. West, *Nature* 418, 754 - 757 (15 Aug 2002). David Snoke, *Nature* 443, 403 - 404 (28 Sep 2006). C. W. Lai, J. Zoch, A. C. Gossard, and D. S. Chemla, *Science* 23 January 2004 303: 503-506. U. Sivan, P. M. Solomon, and H. Shtrikman, *Phys. Rev. Lett.* 68, 1196C1199 (1992). S. De Palo<sup>1\*</sup>, F. Rapisarda<sup>2</sup>, and Gaetano Signore<sup>1</sup>, *Phys. Rev. Lett.* 88, 206401 (2002).

<sup>54</sup> Jinwu Ye, unpublished.

<sup>55</sup> A. H. Castro Neto, Phys. Rev. Lett, 86, 4382 (2001).